Newsletter of the Climate Variability and Predictability Programme (CLIVAR)

Exchanges

Volume 5, No. 3 September 2000

Exchanges No. 17

The challenge of climate research: linking observations and models
Part 1: Ocean data assimilation and state estimation

Study of Tropical Oceans Intercomparison Project (STOIC)

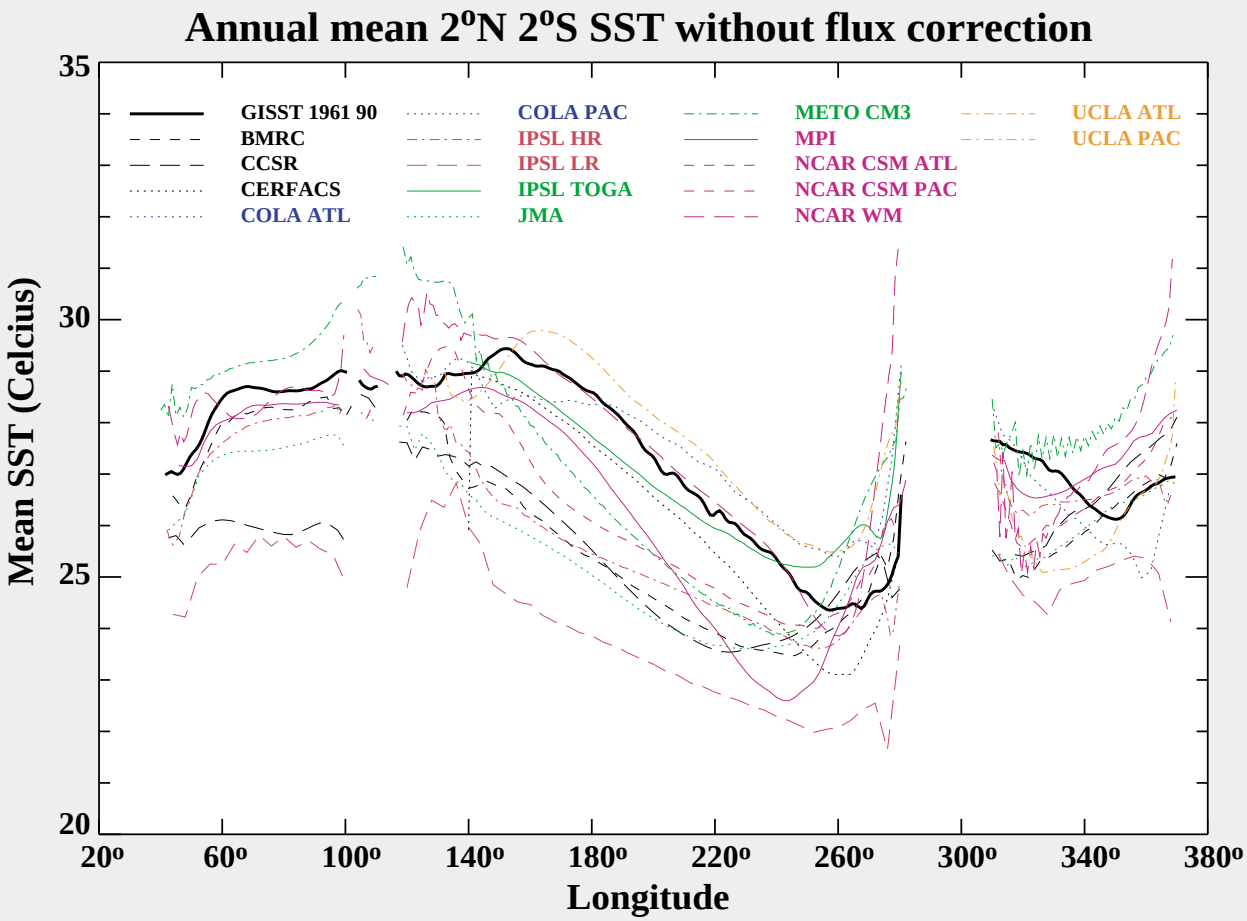

Annual mean SST zonal section for the 2°N-2°S equatorial strip, for observations (GISST3) and for the CGCMs with no tropical flux adjustment(page 21).

More results of the CLIVAR Study of Tropical Oceans Intercomparisons Project (STOIC) can be found in the article by M. Davey et al. on page 21.

Note, that there are also results from the Coupled Model Intercomparison Project (CMIP) and the Paleo Climate Modelling Intercomparison Project (PMIP) in this issue.

International CLIVAR Project Office, Southampton Oceanography Centre, Empress Dock, Southhampton SO14 3ZH, United Kingdom
Tel: +44–23 80 596777, Fax: +44–23 80 596204, icpo@soc.soton.ac.uk, http://www.clivar.org/

Editorial

Dear CLIVAR community,

CLIVAR has global scope. Its complexity is increased by its synthesis of work from several disciplines, notably - meteorology, oceanography, hydrology, paleoclimatology and glaciology. Obervationalists, analysing instrumental as well as proxy data sets, are extending the climate record to provide new insights into today's climate and its relationship to the past. Increasingly realistic climate models enable us to study mechanisms of natural climate variability as well as providing tools for short-term climate predictions and projections of the human influence on climate.

Observationalists and modellers depend on each other and on effective co-operation and communication across the disciplines. Without high quality observations model simulations and climate predictions are of limited use. However observations of all types are sparse and thus CLIVAR requires sophisticated data assimilation and synthesis techniques to bring observations and model simulations together.

Huge reanalysis efforts have already been undertaken and continue to improve our knowledge of the state of the atmosphere over the past decades. In the ocean however such synthesis activities on a global scale are only just beginning. The triggers have been the large amount of in situ data that has been collected throughout the last decades (e.g. under the auspices of WOCE), the availability of global satellite data sets (particularly altimetry) and the development of data assimilation techniques for ocean models. The Global Ocean Data Experiment (GODAE) part of the Global Ocean Observations System (GOOS) and WCRP-CLIVAR is one of the key projects in this context.

We invited the submission of brief articles on the synthesis of data and models to be published in ***Exchanges***. There was an extremely encouraging response that clearly indicated a high level of interest and activity. Indeed the response was so great that we have been unable to include all contributions in a single issue. So we have split the contributions in a thematic way. This issue will mostly cover topics related to the ocean and the next one to be published in December will provide a more atmospheric view. Although this goes against our usual practice of integrating atmosphere and ocean as much as possible it seemed to be the only practical compromise I hope that you will enjoy these two issues.

Finally, I invite you to visit our re-designed web-site at http://www.clivar.org. We believe we have developed a much more user-friendly structure, containing more science and providing useful information for those who are new to CLIVAR as well as to those who are looking for detailed information. We hope that you will enjoy.

John Gould and Andreas Villwock

Preliminary Announcement of Job Vacancies in the International CLIVAR Project Office (ICPO)

In September we expect to advertise internationally for staff scientists to work in the ICPO.

The staff appointed will work as members of the small team of scientists that supports the activities of CLIVAR's panels and working groups and of its Scientific Steering Group. We will be seeking applications from scientists with relevant post-doctoral experience in atmospheric and/or ocean science and from those involved in the study of climate.

Duties will involve

- Developing, implementing and promoting CLIVAR science
- Working with national CLIVAR programmes to assess progress towards (and obstacles to) attaining CLIVAR objectives
- Helping to develop appropriate CLIVAR infrastructure particularly that needed for the effective management and distribution of CLIVAR-relevant data and products
- Identifying and exploiting funding opportunities
- Interacting with related research and operational programmes (e.g. IGBP, GCOS, GOOS, IHDP)
- Providing advice to the Director ICPO in the candidate's area of scientific expertise.

Note - It is expected that the staff appointed will be able to spend up to 20% of their time continuing their own CLIVAR-relevant research activity.

Conditions of employment

A successful candidate will become an employee of the University of Southampton on a salary scale depending on qualification and relevant experience for an initial period of 3 years with the possibility of renewal.

The office is international and therefore candidates from outside the UK are encouraged to apply. Candidates should be able to write and speak English at an adequate level. The job will involve periods of overseas travel.

The ICPO is in the Southampton Oceanography Centre - a modern waterfront laboratory with a vibrant academic research atmosphere.
See **http://www.soc.soton.ac.uk/** for more information.

Please contact the Director ICPO (wjg@soc.soton.ac.uk) if you are interested in working in the ICPO and wish to receive further information.

Ocean state estimation in support of CLIVAR and GODAE

Detlef Stammer for the ECCO Consortium[1]
Scripps Institution for Oceanography, La Jolla, CA, USA
detlef@fjord.ucsd.edu

[1] **D. Stammer (PI), R. Davis, L.-L. Fu, I. Fukumori, R. Giering, T. Lee, J. Marotzke, J. Marshall, D. Menemenlis, P. Niiler, C. Wunsch, V. Zlotnicki**

1. Introduction

The ocean is changing vigorously on a wide range of time and space scales. This variability leads to substantial problems in observing and modelling (simulating) the rapidly changing flow field, the ocean's temperature distribution, and more generally the consequences of those changes for climate. Prototype ocean observing systems, which are now in place as a legacy of programmes such as the World Ocean Circulation Experiment (WOCE) and the Tropical Ocean Global Atmosphere Programme (TOGA), aim at measuring and detecting large-scale changes of various quantities in the ocean, such as temperature, salinity, velocity, nutrients, tracers, etc. The present coverage of interior temperature and salinity measurements will significantly increase with the launch of the global ARGO float programme, which in combination with the complementary high-quality altimetric satellite data will be the backbone of a climate observing system. However, in spite of those unprecedented data, the interior of the ocean will remain fairly undersampled, and much of our understanding and inferences about the ocean's role in shaping our climate will come from the additional information provided by numerical ocean general circulation models.

Among the goals of the present ocean and climate research are therefore to measure, understand, and eventually predict these variations by combining ocean data and ocean models. Today high-resolution simulations of the ocean are performed on a routine basis with realistic coastlines, bottom topography, and surface forcing. By combining ocean observations with those state-of-the-art models, one can obtain an analysis of the time-varying ocean that, when taking into account errors in data and models, must necessarily be more complete and better than the information from either of them alone. This is the heart of ocean state estimation (often referred to as "data assimilation") which has at its goal to obtain the best possible description of the changing ocean by forcing the numerical model solutions to be consistent with the observed ocean conditions. This by itself is a very cost-effective way to obtain a fairly complete description of the changing ocean from a limited set of observations. But at the same time it also identifies model components that need improvement, including surface forcing fields, and guides us as to where we need to extend the observing system to improve the estimated ocean state.

2. Ongoing Activities

Because of the fundamental importance of understanding the present and future states of the ocean, two consortia on ocean modelling and state estimation were supported recently through the US National Ocean Partnership Program (NOPP) with funding provided by the National Aeronautics and Space Administration (NASA), the National Science Foundation (NSF), and the Office of Naval Research (ONR). Those two modelling and assimilation activities are described in detail in Stammer and Chassignet (2000). One of them is called "Estimation of the Circulation and Climate of the Ocean" (ECCO). This ECCO consortium builds on existing efforts at the Massachusetts Institute of Technology (MIT), the Jet Propulsion Laboratory (JPL), and the Scripps Institution of Oceanography (SIO), with additional partners at the Southampton Oceanographic Centre (SOC) and the Max-Planck Institut für Meteorologie (MPI) in Hamburg. Its primary goal is to provide the best possible dynamically consistent estimates of the ocean circulation, which can serve as a basis for studies of elements important to climate (e.g., heat fluxes and variabilities). This model-based synthesis and analysis of the large-scale ocean data set will enable a complete (i.e., including aspects not directly measured) dynamical description of ocean circulation, such as insights into the natures of climate-related ocean variability, major ocean transport pathways, heat and freshwater flux divergences (similar for tracer and oxygen, silica, nitrate), location and rate of ventilation, and of the ocean's response to atmospheric variability.

The ongoing ocean state estimation is based on the MIT GCM (Marshall et al., 1997) and two parallel optimization efforts: the adjoint method (Lagrange multipliers or constrained optimization method), exploiting the Tangent-linear and Adjoint Compiler (TAMC) of Giering and Kaminsky (1997) as described in Marotzke et al. (1999), and a reduced state Kalman filter, e.g., Fukumori et al. (1999). Those data assimilation activities can be summarized as finding a rigorous solution of the model state $\boldsymbol{x}$ over time t that minimizes in a least-squares sense a sum of model-data misfits and deviations from model equations while taking into account the errors in both.

First such results of a global ocean state estimation procedure are summarized in Stammer et al. (2000). Data currently employed in the optimization include the absolute and time-varying T/P data from October 1992 through December 1997, SSH anomalies from the ERS-1 and ERS-2 satellites, monthly mean sea-surface temperature data (Reynolds and Smith, 1994), time-varying NCEP reanalysis fluxes of momentum, heat, freshwater, and NSCAT estimates of wind stress errors. Monthly means of the model state are required to remain within assigned bounds of the monthly mean Levitus et al. (1994) climatology. To bring the model into consistency with the observations, the ini-

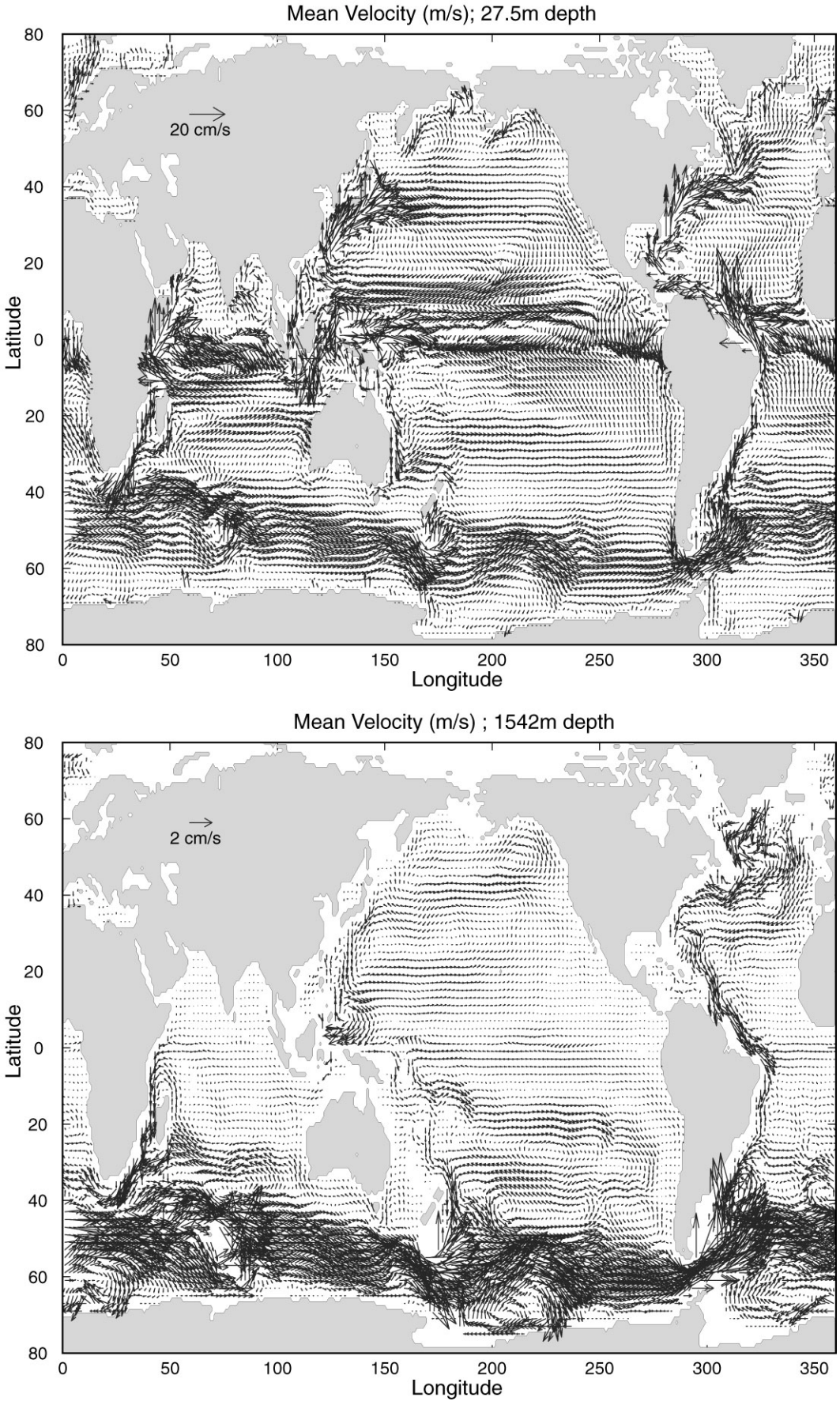

Figure 1: The estimated mean velocity fields at 27 and 1542 m depth show all major current systems. Due to the low model resolution, they are necessarily overly smooth.

tial potential temperature (θ) and salinity (S) fields are modified, as well as the surface forcing fields. Changes in those fields (often referred to as "control" terms) are determined as a best-fit (in a least-squares sense) of the model state to the observations and their uncertainties over the full data period.

A few representative ECCO results are summarised in Fig. 1 and Fig. 2 (page 15). The estimated mean velocity field at 27 and 1542 m depth (Fig. 1) shows all major current systems. But with the low model resolution, they are necessarily overly smooth. The mean net surface heat and freshwater flux fields as they result from the optimization are displayed in the upper row of Fig. 2 (page 15). Their mean change relative to the prior NCEP fields are provided in the middle part of the figure. Ocean transports of all quantities are very energetic and variable. As an example we show here the net northward heat transport across 25°N in the North Atlantic as it results from the optimized model state. The estimated time-varying model state, model transports and consistent surface flux fields will be the basis for a wide variety of climate and societal applications. Many interdisciplinary applications are already under way or have begun recently, including studies of the ocean's impact on the earth angular momentum budget (Ponte et al., 2000).

3. Outlook

Now ongoing computations move toward a 6-year estimate of the time-evolving ocean circulation (1992 through 1997) with 1° spatial resolution that uses all major WOCE data sets as constraints, and that has build in a complete mixed layer model (Large et al., 1994) and an eddy parameterization scheme (Gent and McWilliams, 1990). It is anticipated that, in two to three years, the project will be able to address the US CLIVAR and GODAE related objective of depicting the time-evolving ocean state with spatial resolution up to 1/4° globally and with substantially higher resolution in nested regional approaches which are required for quantitative studies of the ocean circulation. Complementary to this, a 50 year long re-analysis experiment is anticipated but with only a 1°spatial resolution that coincides with the NCEP/NCAR reanalysis period.

A major issue for the ECCO consortium, and generally for the wider oceanographic community, is the way in which the need for computer resources has now outstripped their availability. No short-term solution to the computer resource bottleneck is as yet visible. However, there is an ongoing NOPP activity aiming to organise a substantial increase and improvement in computational infrastructure for oceanographic research (OITI). If successful, it will have a profound impact not only on many future NOPP modelling and assimilation activities; it will be an important step toward reaching GODAE and CLIVAR goals.

The ECCO estimated time-varying model state and consistent surface flux fields from the entire estimation period can be accessed via the web page

http://www.ecco.ucsd.edu/.

References

Fukumori, I., R. Raghunath, L.-L. Fu, and Y. Chao, 1999: Assimilation of TOPEX/POSEIDON altimeter data into a global ocean circulation model: How good are the results? *J. Geophys. Res.*, **104**, 25,647–25,665.

Gent, P. R., and J.C. McWilliams, 1990: Isopycnal mixing in ocean models. *J. Phys. Oceanogr.*, **20**, 150-155.

Giering, R., and T. Kaminsky, 1997: Recipes for adjoint code construction. *ACM Trans. Math. Software*, **24**, 437-474.

Large, W. G., J.C. McWilliams, and S.C. Doney, 1994: Oceanic vertical mixing: a review and a model with nonlocal boundary layer parameterization. *Rev. Geophys.*, **32**, 363–403.

Levitus, S., R. Burgett, and T. Boyer, 1994: *World Ocean Atlas 1994*, vol. 3, Salinity, and vol. 4, Temperature, *NOAA Atlas NESDIS 3 & 4*, U.S. Dep. of Comm., Washington, D.C.

Marotzke, J., R. Giering, Q.K. Zhang, D. Stammer, C.N. Hill, and T. Lee, 1999: Construction of the adjoint MIT ocean general circulation model and application to Atlantic heat transport sensitivity. *J. Geophys. Res.*, **104**, 29,529 - 29,548.

Marshall, J., A. Adcroft, C. Hill, L. Perelman, and C. Heisey, 1997a: A finite-volume, incompressible navier-stokes model for studies of the ocean on parallel computers. *J. Geophys.* Res., **102**, 5753–5766.

Ponte, R. M., D. Stammer, and C. Wunsch, 2000: Improved ocean angular momentum estimates using an ocean model constrained by large-scale data. *Geophys. Res. Lett.*, submitted.

Reynolds, R. W., and T.M. Smith, 1994: Improved global sea surface temperature analyses using optimum interpolation. *J. Climate*, **7**, 929–948.

Stammer, D., and E.P. Chassignet, 2000: Ocean State Estimation and Prediction in Support of Oceanographic Research. *Oceanography*, **13**, 51–56.

Stammer, D., C. Wunsch, R. Giering, C. Eckert, P. Heimbach, J. Marotzke, A. Adcroft, C.N. Hill, and J. Marshall, 2000: The global ocean circulation and transports during 1992 –1997, estimated from ocean observations and a general circulation model, in preparation.

Design of an array of profiling floats in the North Atlantic from model simulations - Preliminary results -

Stephanie Guinehut, Gilles Larnicol, and Pierre-Yves Le Traon
CLS Space Oceanography Division, Ramonville St Agne, France
stephanie.guinehut@cls.fr

1. Introduction

The aim of the study is to analyse the contribution of different profiling float arrays [as proposed by the *Argo* project (Roemmich at al., 1999)] to the description of the variations of the large scale and low frequency 3-D thermohaline fields. It uses outputs and profiling float simulations from a primitive equation model of the North Atlantic Ocean.

2. Data and Method

2.1. Data

Model outputs and profiling float simulations from the MERCATOR project (Blanchet et al., 1999) are used. The model is a primitive equation model of the North Atlantic Ocean with a 1/3-degree horizontal resolution and 43 vertical levels. It uses realistic forcing from ECMWF reanalysis. The 1989-year simulation is used for the study.

2.2. Method

The objective is to reconstruct the large scale and low frequency variability of the temperature (T) and salinity (S) fields at different depths from simulated T and S profiles corresponding to three-degree ("nominal" *Argo* resolution) Eulerian and Lagrangian arrays. The main issue is to analyze how an a priori defined large scale signal can be mapped from sparse measurements with a low signal-to-noise ratio (mainly due to mesoscale variability).

2.2.1. The reference fields

The first step consists in calculating the model large scale reference fields at different depths. Anomalies of the T and S fields relative to a five-year mean (1989 – 1993) are first calculated at each depth. The anomalies are then separated into a large scale part and a "mesoscale" part using a 2D Loess smoother (Greenslade et al., 1997) with a cut-off wavelength of 10° in latitude and longitude. This approximately corresponds to averages over 6° by 6° boxes (Greenslade et al., 1997) and is supposed to be representative of signals which can be mapped from a global profiling float array. An example is given in Figure 1 (page 16) for an instantaneous field of T at 200 m. The filter appears to preserve the main large scale features of the T and S fields while mainly removing the mesoscale signals. The large scale signal is the reference field which we want to reconstruct.

2.2.2. The objective analysis method

Simulated T and S profiles corresponding to three-degree Eulerian and Lagrangian arrays are subsampled from the model fields every ten days and at different depths (20, 200 and 1000 m). An objective analysis method (Bretherton et al., 1976) is then used to reconstruct the large scale signal variations from these simulated data.

The covariance functions of the large scale T and S signals at different depths are derived on a one degree by one degree grid from the analysis of the model large scale fields over the year 1989 (see figure 1-b). The model mesoscale signal (see figure 1-c) is used to determine the noise-to-signal ratio on the same grid. Thus, both covariance and noise-to-signal ratio depend on the geographical position and on the depth. Values are very similar for the T and S fields. Near the sea surface (20 m), the large scale signal dominates with low noise-to-signal ratios. Below the mixed layer depth, the large scale signal is, however, much smaller and the noise-to-signal ratio increases considerably. The noise-to-signal ratio varies from 0.1 at 20 m to 10 at 1000 m.

The analyses are performed every ten days over a one-year period (year 1989) but since the objective is to retrieve the low frequency variability of the large scale signal, monthly means are calculated. They are then compared to the monthly means derived from the model large scale reference fields.

3. Some statistical results for a three-degree Eulerian array

A three-degree regular Eulerian array (530 profiling floats over the area) is first tested for the T and S fields at 20, 200 and 1000 m. As an example, Figure 2 (page 16) shows the rms of the monthly means of the large scale T signal at 200 m and the rms of the mapping error obtained with the three-degree array. The rms of the mapping error is almost everywhere much smaller than the rms of the signal. The three-degree array captures the main large scale signal

Table 1 compares the mean mapping error (in rms and in percentage of signal variance) of the monthly means of the large scale T and S fields at different depths. Near the sea surface (20 m), the T field is a very large scale signal with a large variance (rms = 2.08 °C). It corresponds to the SST response to the (large scale) atmospheric heat fluxes. This signal is almost perfectly retrieved with the three-degree array (99 % of the variance). The errors on the T signals decrease with depth (0.16 °C at 20 m to 0.14 °C at 200 m and 0.05 °C at 1000 m) but the T variance decreases much more rapidly (2.08 °C, 0.34 °C and 0.08 °C respectively at the same depths). As a result, the error relative to the signal variance increases considerably with depth. The

Field	Rms of mapping error (°C)	Mapping error in % of signal variance
	Temperature	
20 m (2.08 °C)	0.16	0.6
200 m (0.34 °C)	0.14	17.5
1000 m (0.08 °C)	0.05	34.4
	Salinity	
20 m (0.19 psu)	0.05	7.4
200 m (0.06 psu)	0.02	15.8
1000 m (0.01 psu)	0.008	28.3

Table 1: Mapping errors of the monthly means of the large scale temperature and salinity fields at different depths for the three-degree array (530 floats). The rms of the T and S signals are also indicated.

three-degree array captures the main large scale signal at 200 m (82 % of the signal retrieved) but only 66% of the signal variance at 1000 m (table 1) due to the very low temperature variance at this depth. Results obtained for the S field are very similar to those obtained with the T field at 200 and 1000 m. Near the sea surface, salinity spatial scales are smaller than temperature ones and the signals are less easily reconstructed.

4. Comparison of Eulerian and Lagrangian arrays

Differences between Eulerian and Lagrangian three-degree arrays are now analysed. We used the Lagrangian float simulations at a 500 m depth. We chose to analyse the 500 m simulations (rather than 2000 m) to have a sufficient (and probably more realistic) estimation of the actual dispersion of the floats.

The time evolution of the T mapping error at 200 m shows only a slight degradation of results for the Lagrangian array compared to the Eulerian array (not shown). Differences are of the order of 0.01 °C which is small compared to the signal variance. In only one year, the profiling floats did not disperse/converge much and all the floats continue to provide useful information. Part of the differences can actually be explained by the loss of 20 floats (which left the model domain) during this year.

Array	Rms of mapping error (°C)	Mapping error in % of signal variance
T at 200 m - signal variance = 0.34 °C		
*3°*3° Eulerian*	0.14	17.6
*3°*3° Lagrangian*	0.15	20.1

Table 2: Mapping errors of the monthly means of the large scale temperature field at 200 m for the three-degree Eulerian and Lagrangian arrays.

5. Conclusions and perspectives

The study suggests that a three-degree array of profiling floats cycling every 10 days can retrieve most of the variance of the large scale and low frequency T and S signals as observed by a 1/3° primitive equation model. More than 90 % of the variance of the T and S signals is retrieved at the surface (20 m), 80% at 200 m and between 65 and 70 % at 1000 m. Comparison between Eulerian and Lagrangian arrays shows only a slight degradation of the results due to the dispersion of floats.

These results depend, of course, on the a priori definition of the large scale and low frequency signal (here space/time means over approximately 6°x 6° boxes and 1 month). Sensitivity studies to this a priori choice should be carried out to determine the mapping accuracy according to the space (e.g. from 3 degrees to 10 degrees) and time (e.g. from 10 days to one year) scales of signals to be mapped. Higher resolution models should also be used to better estimate the impact of the mesoscale field on the large scale signal retrieval. Finally, floats simulations over longer periods (4 years) should be used to better estimate the impact of the Lagrangian dispersion of the floats during their expected life-time.

Note, finally, that only profiling float data were used here to estimate the large scale T and S fields. It is clear, however, that in the future the best use of profiling float data will be when they are combined with other data sets and models through effective data assimilation techniques. The development and application of such techniques is the main (challenging) objective of GODAE (Smith and Lefebvre, 1997). The combination of profiling float data with satellite altimetry will be, in particular, very instrumental in reducing the aliasing due to the mesoscale variability.

Acknowledgements

We thank the MERCATOR PAM team for providing us with the model simulations. The study was partly funded by CNES under contract CNES/CLS 794/99/7805/00.

References

Blanchet, I., T. De Prada, Y. Drillet, L. Fleury, H. Perez, L. Siefridt, and B. Tranchant, 1999: The North Atlantic / Mediterranean Mercator Prototype. *Oceanobs99. Conference proceedings, St Raphael.*

Bretherton, F., R.E. Davis, and C.B. Fandry, 1976: A technique for objective analysis and design of oceanographic experiments applied to MODE-73. *Deep-Sea Res.*, ***23***, *559-582.*

Greenslade D.J.M., D.B. Chelton, and M.G. Schlax, 1997: The midlatitude resolution capability of sea level fields constructed from single and multiple satellite altimeter datasets. *J. Atmos. &Oceanic. Technol.*, ***14***, *849-870.*

Roemmich, D., O. Boebel, Y. Desaubies, H. Freeland, B. King, P.-Y. LeTraon, B. Molinari B. Owens, S. Riser, U. Send, K. Takeuchi, and S. Wijffels, 1999: *Argo*: The Global Array of Profiling Floats. *Oceanobs99. Conference Proceedings*, *St Raphael.*

Smith, N., and M. Lefebvre, 1997:"The Global Ocean Data Assimilation Experiment" (GODAE). *Monitoring the oceans in the 2000s : an integrated approach*, *International Symposium*, Biarritz, October 15-17. 1997.

Assimilation of Topex/Poseidon data improves ENSO hindcast skill

Sigrid Schöttle and Mojib Latif,
Max-Planck-Institut für Meteorologie, Hamburg, Germany
schoettle@dkrz.de

Introduction

Successful El Niño forecasts depend on the availability of suitable ocean initial states, especially from subsurface layers. Sea surface heights contain information about the ocean interior, and they can be measured with high accuracy from space. Here, we investigate the effect of the assimilation of TOPEX/POSEIDON sea surface heights on the oceanic initial conditions and the El Niño hindcast skill.

Several methods were developed to assimilate the sea surface heights (Cooper and Haines, 1996; Segschneider et al., 1999; Verron et al., 1999). Here we use an empirical method to project the sea surface heights on the vertical modes of the system. We have conducted an ensemble of El Niño hindcasts and forecasts with a hybrid coupled model. Our latest forecasts indicate the development of a weak El Niño towards the end of this year.

Models

Our forecast system consists of a hybrid coupled ocean-atmosphere model (HCM) and an ocean assimilation scheme described below. The ocean component of the HCM is a Pacific version of the HOPE-E model (Wolff et al., 1997), an ocean general circulation model based on primitive equations. Further details of the ocean model can be found in Venzke et al. (2000). The atmospheric component of the HCM is a statistical model (Barnett et al., 1993) which has been derived from a regression analysis of sea surface temperature and surface wind stress anomalies.

Forcing

The ocean model was forced by heat fluxes and wind stresses of two different data sets: a) NCEP reanalysis (Kalnay et al., 1996) for the period 1973-1997 and b) ECMWF re-analysis (ERA) and ECMWF operational analysis for the period 1990-June 2000. For the model runs with assimilation we used Topex/Poseidon data provided by CLS (Collecte Localisation Satellite). These data were already corrected and mapped (Le Traon et al., 1998). Up to January 2000 we used historical homogeneous data on 10 day maps. Thereafter near real time data on 7 day maps were used which are available one week after their measurement.

Assimilation method

The assimilation method is similar to those of Fischer et al. (1997) and Mellor and Ezer (1991). Our approach consists of two steps. In the first step, the altimeter data were projected from the surface onto the vertical temperature structure at each grid point. This projection was realised by applying a transfer function that was computed from a regression between the sea level anomalies (SLA) and the principal components of the first two empirical orthogonal functions of the vertical temperature anomaly (TA) profile. The SLA and TA used to compute the regression were taken from a 45 year ocean model run forced by observations. After the projection a mean seasonal cycle was added to yield full temperatures. In the second step, the model temperatures were nudged to these full temperatures at each time step with a relaxation time of about 4 days.

Results

Hindcasts were started every three months for the period 1993 to 1997. Sets of hindcasts were performed with and without assimilation of Topex/Poseidon data. Correlation coefficients of sea surface temperature anomalies (SSTA) averaged over the Niño-3 region were calculated between observations and hindcasts for time lags of 1 to 6 months (Fig.1). The assimilation of Topex/Poseidon data improved the skill of El Niño hindcasts considerably at all time lags.

Our ocean analysis obtained by assimilating the Topex/Poseidon sea surface heights shows in June 2000 positive temperature anomalies at subsurface levels in the western equatorial Pacific. These are similar in magnitude to those simulated in December 1996 (Fig. 2). The anomalies in June 2000, however, are located slightly farther west relative to those in December 1996. We initialised forecasts in November 1999 and February, May and June 2000. Each forecast has a duration of 12 months. The results in terms of the Niño-3 SST index are shown in Fig. 3. The HCM predicts a mild El Nino for the winter season 2000/2001. One should keep in mind, however, that the model's skill drops rapidly beyond lead times of 6 months.

In summary, we can conclude that the assimilation of Topex/Poseidon sea surface heights improves significantly the skill of ENSO hindcasts. Future studies will involve the application of more sophisticated assimilation schemes and the inclusion of additional observations such as those measured by the TOGA-TAO array.

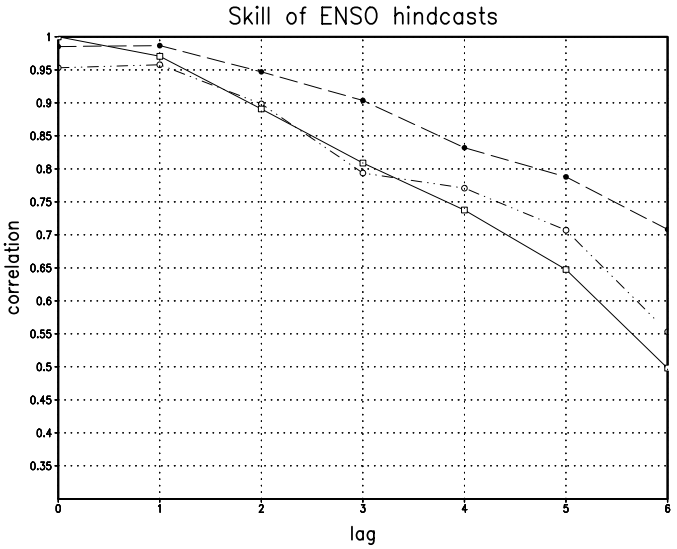

Fig. 1: Hindcast skill of Niño-3 SSTA index of a) persistence (black line), b) hindcasts without assimilation of T/P data (dashed dotted line) and c) hindcasts with assimilation of T/P data (dashed line).

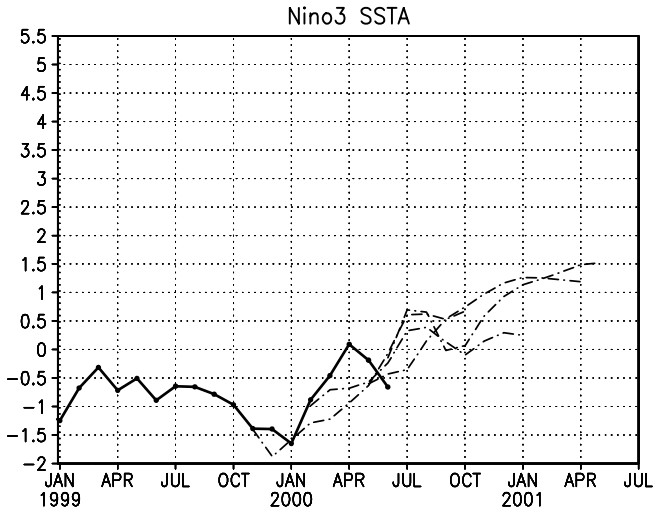

Fig. 3: Niño-3 SSTA index of a) ECMWF SSTA data (black line) and forecasts initialised from an ocean model assimilation run (dashed-dot lines).

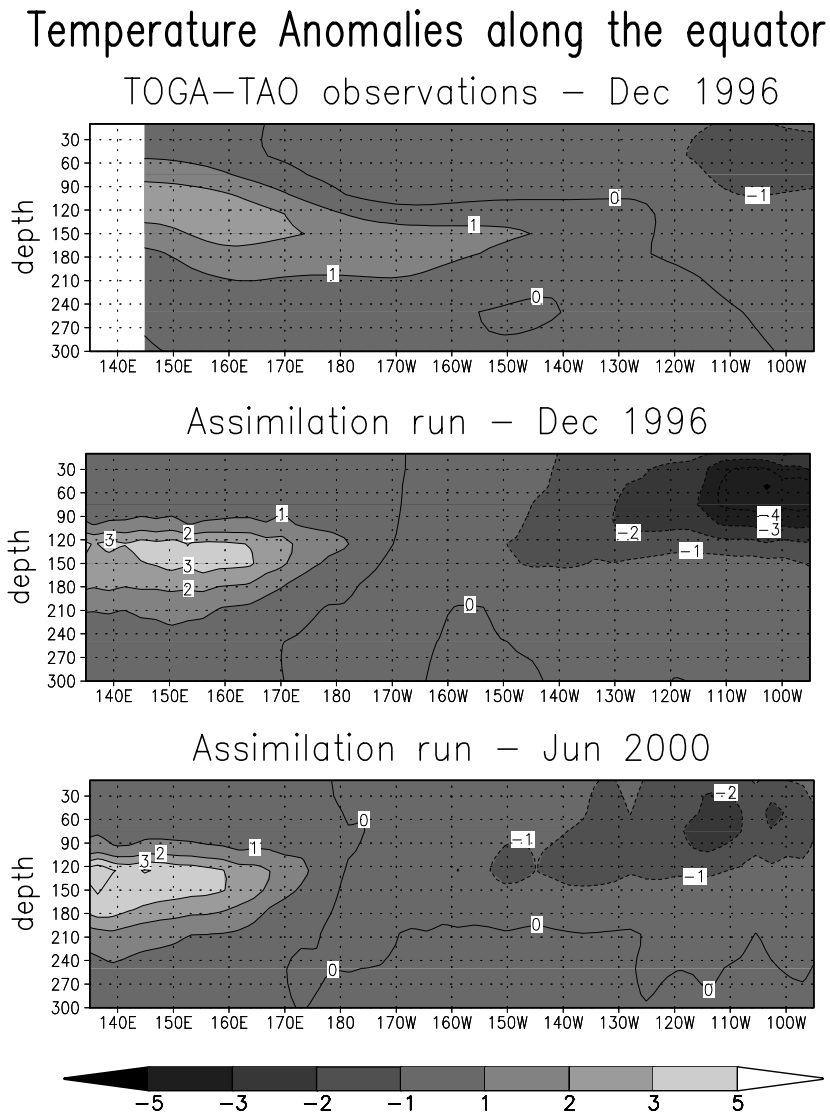

Fig. 2: Longitude - depth sections of observed temperature anomalies in December 1996 (top), model experiment with data assimilation for th same period (middle) and model conditions for June 2000, used for the latest forecast.

Acknowledgements

The altimeter products were produced by the CLS Space Oceanography Division as part of the DUACS (ENV4-CT96-0357) project. We thank M. Balmaseda for providing us with the ECMWF forcing data.

References

Barnett, T.P., M. Latif, N. Graham, M. Flügel, S. Pazan and W. White, 1992: ENSO and ENSO-related predictability. Part I: Prediction of equatorial Pacific sea surface temperature with a hybrid coupled ocean-atmosphere model. *J. Climate*, **7**, 1513-1564.

Cooper, M., and K. Haines, 1996: Altimetric assimilation with water property conservation. *J. Geophys. Res.*, **101**, 1059-1077.

Fischer, M., M. Flügel, M. Ji, and M. Latif, 1997: The Impact of Data Assimilation on ENSO Simulations and Predictions. *Mon. Wea. Rev.*, **125**, 819-829.

Kalnay, E., M. Kanamitsu, R. Kistler, W. Collins, D. Deaven, L. Gandin, M. Iredell, S. Saha, G.White, J. Woollen, Y. Zhu, A. Leetma, R. Reynolds, M. Chelliah, W. Ebisuzaki, W. Higgins, J. Janowiak, K.C. Mo, C. Ropelewski, J. Wang, R. Jenne, and D. Joseph, 1996: The NCEP/NCAR 40-Year Reanalysis Project, *Bull. Am. Meteor. Soc.*, **77** , 437-471.

Le Traon, P.Y., F. Nadal, and N. Ducet, 1998: An improved mapping method of multi-satellite altimeter data. *J. of Atmos. & Oceanic Tech.*, **15**, 522-534.

Mellor, G.L., and T. Ezer, 1991: A Gulf stream model and an altimeter assimilation scheme. *J. Geophys. Res.*, **96**, 8779-8795.

Segschneider, J., J. Alves, D.L.T. Anderson, M. Balmaseda, and T.N. Stockdale, 1999: Assimilation of TOPEX/Poseidon data into a seasonal forecast system. *Phys. Chem. Earth (A)*, **24**, 369-374.

Verron, J., L. Gourdeau, D.T. Pham, R. Murtugudde, A.J. Busalacchi, 1999: An extended Kalman filter to assimilate satellite altimeter data into a non-linear numerical model of the Tropical Pacific: method and validation, J. *Geophys. Res.*, **104**, 5441-5458.

Wolff, J.O., E. Maier-Reimer, and S. Legutke, 1997: The Hamburg Ocean Primitive Equation Model. Deutsches Klimarechenzentrum, Hamburg, *Technical Report*, **13**, 98pp.

The impact of TOPEX/POSEIDON altimetry assimilation on equatorial circulation modelling in the Pacific

Howard F. Seidel, Texas A&M University, College Station, TX, USA
hseidel@ocean.tamu.edu
Benjamin Giese, Texas A&M University, College Station, TX, USA
Jim Carton, U. Maryland, College Park, MD, USA

Abstract

A medium resolution ocean general circulation model (OGCM) is used to explore current structure and variability in the equatorial Pacific for the period from 1992-1997. The model assimilates surface and subsurface temperature data from expendable bathythermographs (XBT), the Tropical Ocean Global Atmosphere-Tropical Atmosphere-Ocean (TOGA-TAO) moorings and altimetry data from the TOPEX/Poseidon satellite. Model experiments are run with and without the assimilation of TOPEX/Poseidon altimetry observations in order to study their impact on model currents. Assimilated currents are compared with observed currents from the TOGA-TAO moorings at 110°W, 140°W and 165°E. Since mooring data are not assimilated, these data provide an independent verification of the model results. The comparison shows that the model produces accurate equatorial currents over a wide range of spatial and temporal scales. In particular, the model correctly resolves temporal variability from instability waves with periods of less than a month to interannual changes with periods of several years. A statistical analysis is conducted to quantify the model's skill in producing accurate currents and to evaluate the importance of TOPEX/Poseidon altimetry assimilation.

Model Description

The model used is an intermediate resolution version of the Modular Ocean Model 3 (MOM3) code developed at the National Oceanic and Atmospheric Administration's Geophysical Fluid Dynamics Laboratory Pacanowski, 1995. The model's spatial domain incorporates the Pacific basin from 120°E to 70°W and from 30°S to 30°N. The grid resolution varies over the domain with the highest resolution in the eastern equatorial region. The longitudinal resolution is a constant 0.5° from the eastern boundary to 140°W. From 140°W to the western boundary the longitudinal resolution increases from 0.5° to 1.5° . The latitudinal resolution is a constant 0.5° from 5°S to 15°N, expanding poleward of this region to 1.5° at the southern and northern boundaries. The resulting grid contains 241 points in longitude and 82 points in latitude. The model has 20 vertical layers with 10 equally spaced levels in the upper 150 meters. The model time step is one hour. The model employs a Richardson number dependent mixing scheme in the vertical and a biharmonic mixing scheme in the horizontal. The model incorporates an optimal interpolation scheme which assimilates expendable bathythermograph (XBT) and mechanical bathythermograph (MBT) temperature data from the NODC Levitus and Boyer (1994) data set, thermister data from the TOGA-TAO array of moorings in the Pacific and TOPEX/Poseidon satellite altimetry data when it became available in September 1992. The assimilation scheme and its incorporation into the model is described in detail by Carton et al., 1996. The model is forced with weekly NCEP winds Kalnay et al., 1996. Sea surface temperature (SST) is damped to NCEP weekly values and the sea surface salinity (SSS) is damped to monthly

mean climatology from the comprehensive ocean atmosphere data set (COADS) Dasilva et al., 1994. The model was spun up from 1985 to 1991 using data assimilation of XBT, MBT and TOGA-TAO temperature data. This paper presents the results of two model runs. The first run includes the assimilation of all of the observations listed above. The second run assimilates the temperature observations but does not include the TOPEX/Poseidon altimetry observations.

Verification of Assimilated Currents Against TOGA-TAO Observations

Current meter data are available at several depths from the equatorial TOGA-TAO moorings at 110°W, 140°W and 165°E. These data are compared to model output from the run that includes Topex/Poseidon altimetry data to verify model performance. Plots of these comparisons at 10 and 120 m at 140°W are shown in Figures 1a and 1b (page 12) . For these plots the observed currents have been time averaged over 5 days to match the model output. No manipulation has been performed on the model output. The plot at 10 m (Figure1a) shows the model's ability to capture zonal current variability over a wide range of time scales. Both the phase and the magnitude of high frequency instability waves agree well with the observations. The seasonal variations of the zonal current and of the instability wave energy can be easily identified in these plots. The passage of two equatorial Kelvin waves at 140°W in early 1997 associated with the 1997-1998 El Niño is also clearly visible. The plot of zonal current at 120 m (Figure 1b) demonstrates the ability of the model to accurately simulate the Equatorial Undercurrent (EUC) throughout the assimilation period except for the first few months of the model run during a period prior to the availability of altimery observations. The model has captured both the mean velocity and the variability of the EUC. The shutdown of the EUC associated with the 1997-1998 El Niño is well simulated by the model during the first half of 1997. A statistical analysis of all depths for which current meter data is available is presented in Table 1. At 110°W the correlations (with Topex) range from a high of 0.71 at 45 m to a low of 0.41 at 80 m at 140°W. The highest value at 140°W is 0.79 at 120 m and the lowest value is 0.38 at 200 m. The current meter data available at 110°W covers 63% of the time period presented and at 140°W it covers 77%. At 165°E the current meter data only covers 38% of the time period.

The Contribution of TOPEX/Poseidon

The impact of the TOPEX/Poseidon assimilation at 140° W is presented in Figures 1c and 1d. In these figures the output from the model run that includes TOPEX/Poseidon assimilation is plotted along with the run that assimilates only XBTs and TOGA-TAO temperature data but not Topex/Poseidon altimetry data. It is evident that the addition of the TOPEX/Poseidon altimetry observations improves the ability of the model to properly represent the phase of the tropical instability waves (TIWs). In Figure 1a the TIWs during the 1995 and 1996 seasons are in phase with the observations. In Figure 1c the TIWs from the run without altimetry assimilation are out of phase with the run including altimetry assimilation. During the 1996 season the run without altimetry assimilation completely misses one wave during December. The assimilation of altimetry also helps correct model biases. The zonal currents plotted in Figure 1b very accurately reproduces the strength of the EUC at 140°W as observed by the TOGA-TAO current meter. The zonal current at 120 m from the run without altimetry assimilation (2d) is consistently 20 - 40 cm s^{-1} weaker than the observations.

Table I. Statistical comparison of model (with and without Topex assimilation) and observed zonal currents at 110°W, 140°W and 165°E.

Longitude	Depth	With Topex		Without Topex	
		RMS diff[1]	Correlation	RMS diff[1]	Correlation
	(meters)	*(cm s^{-1})*		*(cm s^{-1})*	
110°W	10	34	**0.66**	41	**0.55**
	25	31	**0.70**	35	**0.64**
	45	30	**0.71**	31	**0.69**
	80	22	**0.41**	25	**0.33**
	120	18	**0.61**	21	**0.48**
	200	12	**0.70**	21	**0.24**
140°W	10	33	**0.61**	36	**0.54**
	25	28	**0.64**	30	**0.61**
	45	33	**0.59**	38	**0.51**
	80	29	**0.58**	31	**0.56**
	120	13	**0.79**	21	**0.63**
	200	14	**0.38**	24	0.10
165°E	10	40	**0.61**	42	**0.51**
	50	34	**0.21**	39	0.08
	100	28	**0.59**	30	**0.55**
	150	21	0.17	21	**0.31**
	200	22	**0.69**	26	**0.63**
	250	15	**0.40**	17	**0.45**

Correlations in **bold** are above the 99% significance level.

[1]Computed after removing the mean from the observations and the model data.

The statistical analysis presented in Table 1 quantifies the contribution of altimetry assimilation at other longitudes and depths. The correlations between the modelled currents (with and without TOPEX/Poseidon) and observations are presented. In general, the inclusion of altimetry observations increases the correlation values by about 0.1. The analysis and verification of the model run that includes TOPEX/Poseidon assimilation are covered in detail by Seidel and Giese (1999).

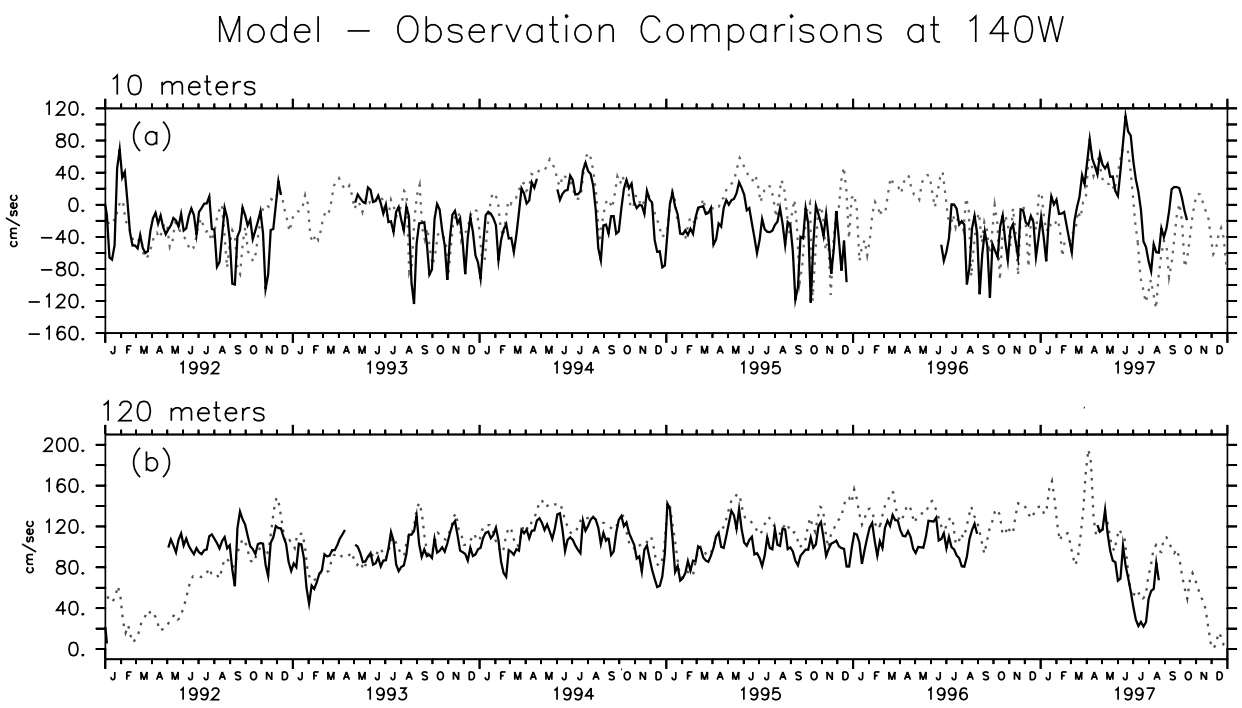

Heavy line - Observations, Dotted line - Model with TOPEX Assimilation

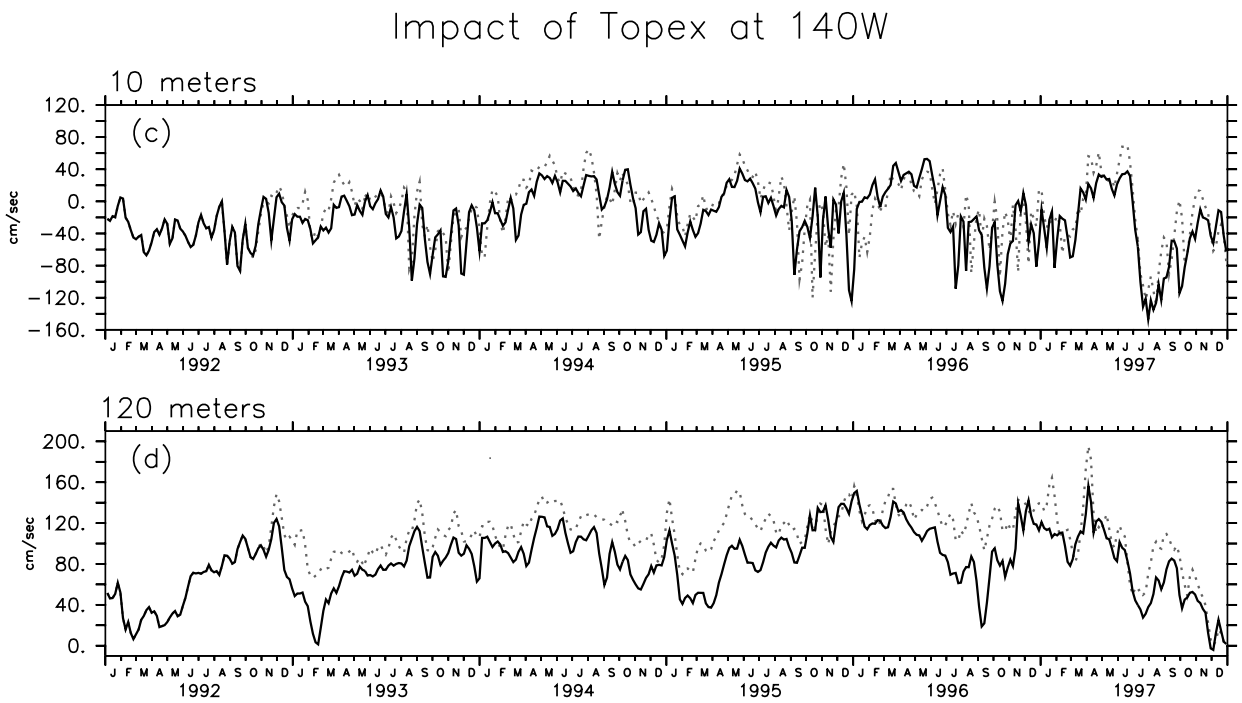

Heavy line - Model without TOPEX Assimilation, Dotted line - Model with TOPEX Assimilation

Figure 1: Model - observations comparisons at 140°W (upper) and impact of TOPEX at 140°W (lower)

Conclusions

In general, the assimilating model shows good skill in reproducing ocean currents on the equator where mooring data are available at 110°W, 140°W and 165°E. The contribution of TOPEX/Poseidon altimetry data is the addition of phase information in the TIW region and a correction of model biases at depth. Statistically this improves the correlation between model zonal currents and observations by about 0.1. We plan to use a global version of this model coupled with an atmospheric model to investigate its value in climate prediction.

References

Carton, J. A., B.S. Giese, X. Cao, and L. Miller, 1996: Impact of altimeter, thermistor, and expendable bathythermograph data on retrospective analyses of the tropical Pacifc Ocean. *J. Geophys. Res.*, **101**, 14,147-14,159.

da Silva, A. M., C. C. Young, and S. Levitus, 1994: Atlas of Surface Marine Data 1994, Vol. 1, Algorithms and Procedures. *Tech. Rep.* **6**, Natl. Oceanic and Atmos. Admin., Silver Spring, Md.

Kalnay, E., M. Kanamitsu, R. Kistler, W. Collins, D. Deaven, L. Gandin, M. Iredell, S. Saha, G. White, J. Woollen, Y. Zhu, A. Leetma, R. Reynolds, M. Chelliah, W. Ebisuzaki, W. Higgins, J. Janowiak, K.C. Mo, C. Ropelewski, J. Wang, R. Jenne, and D. Joseph, 1996: The NCEP/NCAR 40-year reanalysis project. *Bull. Am. Meteor. Soc.*, **77** , 437-471.

Levitus, S., and T. Boyer, 1994: World Ocean Atlas 1994, Vol. 4, Temperatur. Technical Report No. 4 , U. S. Department of Commerce,Washington, D.C.

Pacanowski, R., 1995: MOM 2 documentation: User's guide and reference manual. Tech. Rep. 3 , Geophys. Fluid Dyn. Lab., Princeton, N.J.

Seidel, H.F., and B.S. Giese, 1999: Equatorial currents in the Pacific Ocean 1992-1997. *J. Geophys. Res.*, **104**, 7849-7863.

Impact of temperature error models in a univariate ocean data assimilation system

Michael K. Tippett
International Research Institute for Climate Prediction, Palisades, NY, USA
tippett@iri.ldgo.columbia.edu

Ming Ji
CMB, NCEP, Camp Springs, MD, USA

Alexey Kaplan
Lamont-Doherty Earth Observatory of Columbia University, Palisades, NY, USA

Introduction

Ocean data assimilation systems combine observations with information from prediction models to produce an analysis or estimate of the ocean state. Statistical interpolation assimilation methods use observations to correct a model-based first guess and require specification of first-guess and observation error statistics. Often the first-guess error covariance (FGEC) is described by an analytical covariance function whose structure is not directly related to ocean dynamics. On the other hand, ensemble and reduced-space methods represent the FGEC by a low-rank approximation coming from the dynamical model. Here we examine the impact of adding a low-rank FGEC component to an operational univariate ocean data assimilation (ODA) system. Small-scale structures are eliminated from the mean temperature correction and positive impact is seen in the zonal currents.

Ocean data assimilation system

The ODA system uses the MOM-1 Pacific basin model with TAO, XBT and blended SST observations as described in (Behringer et al., 1998). At each assimilation time, the model first-guess is compared to observations and a temperature correction is calculated by minimizing a cost function (Derber and Rosati, 1989). The cost function rewards, with weight depending on the observation error covariance, temperature corrections that reduce mismatch between analysis and observations. Simultaneously, temperature corrections whose magnitude and spatial structure are incompatible with the FGEC are penalized. The spatial structure of the FGEC controls how first-guess errors are corrected in a neighbourhood of the observation, an important property when there are few observations.

Assimilation experiments

We compare a control analysis with one obtained using a FGEC model with low-rank component. The control analysis is produced using a FGEC model G^f with Gaussian horizontal correlations and temperature gradient dependent vertical correlations (Behringer et al., 1998). The reduced-space FGEC S^f has the form:

$$S^f = \alpha G^f_{\perp} + ZFZ^T = \alpha(I - ZZ^T)G^f(I - ZZ^T) + ZFZ^T \qquad (1)$$

where $0 \le \alpha \le 1$ is a tunable parameter, the columns of the matrix Z are the EOFs of a simulation and F is a symmetric positive definite matrix. This formulation, like that of Hamill and Snyder (2000) is simple to implement in an existing 3D-Var system; in this formulation however, we assume the reduced-space and analytical parts to be uncorrelated. For the special case $\alpha = 0$ whose results are presented here, calculation of the temperature correction is simplified. We consider the period March, 1993 - February, 1997 and use the reduced-space spanned by the first 80 EOFs.

Results

The mean temperature correction and the mean difference between observations and analysis are significantly

different from zero, indicating systematic biases (Fig. 1, page 17). The reduced-space analysis is generally less constrained by observations than the control analysis. In both cases, the mean temperature correction is correlated with the mismatch between analysis and TAO data. In the control analysis, the mean temperature correction maxima and minima correspond to TAO locations, producing structures with length-scales on the order of the TAO mooring spacing. These structures do not appear in the analysed temperature field or its derivatives. In the reduced-space experiment, the mean temperature correction attempts to correct the same model and forcing deficiencies but does so with larger scale structures. In both experiments the impact on the analysed temperature fields (compared to simulation) is qualitatively similar. However, the impacts on the zonal currents are different (Fig. 2, page 17). The mean zonal surface current exceeds -50 cm/sec. in the Eastern Pacific for the control case while the measured value at (0^oN,110^oW) is -17.3 cm/sec. The equatorial undercurrent core in the control is weakened by about 12 cm/sec and shifted to the west compared to the reduced-space experiment. Similar impacts on zonal velocity are seen when simulations are forced with time-independent mean temperature corrections.

Conclusions

Temperature error models in univariate ocean data assimilation systems impact zonal velocity. The temperature corrections produced using a reduced-space FGEC have less small-scale structure and were seen to have a positive impact on zonal currents.

In the reduced-space FGEC model used here ($\alpha = 0$), errors are reduced only on the reduced-space which in the reduced-space Kalman filter causes divergence (Cohn and Todling, 1996). The choice here of simulation EOFs to span the reduced subspace is not necessarily appropriate even in the most idealized systems since the simulation EOFs do not include the effect of data assimilation or model error (Tippett et al., 2000). Therefore, likely there is benefit in considering a FGEC with both reduced and analytical parts ($a>0$). Future work will examine impact on forecast skill.

References

Behringer, D. W., M. Ji, and A. Leetmaa, 1998: An improved coupled model for ENSO prediction and implications for ocean initialization. Part I: The ocean data assimilation system. *J. Climate*, **126**, 1013-1021.

Cohn, S. E., and R. Todling, 1996: Approximate data assimilation schemes for stable and unstable dynamics. *J. Meteor. Soc. Japan*, **74**, 63-75.

Derber, J., and A. Rosati, 1989: A global oceanic data assimilation system. *J. Phys. Oceanogr.* **9**, 1333-1347.

Hamill, T.M., and C. Snyder, 2000: A hybrid ensemble Kalman filter/ 3D-variational analysis scheme. *Mon. Wea. Rev.*, in press.

Tippett, M.K., S.E. Cohn, R. Todling, and D. Marchesin, 2000: Low-dimensional representation of error covariance. *Tellus*, in press.

Variational assimilation of SSH variance from TOPEX/POSEIDON and ERS1 into an eddy-permitting model of the North Atlantic

Armin Köhl, Scripps Institution of Oceanography, La Jolla, CA, USA
akoehl@ucsd.edu

Jürgen Willebrand, Institut für Meereskunde, Kiel, Germany
jwillebrand@ifm.uni-kiel.de

Two categories of methods are available for the assimilation of altimeter data. Due to the lack of a precise geoid, application of the sequential method use an additional independent data source for the mean sea surface height since the method is incapable to change the mean state consistent with the assimilated anomalies (The DYNAMO Group, 1997). The adjoint method searches for an optimal trajectory that by construction represents the data in a dynamically consistent way. The method, however, is due to the use of tangent linear equations in high resolution models useful only on very short time spans of a few months, where the linear approximation holds. Such short periods are not sufficient for a significant transfer of informations into depth.

We present an approach for an adjoint method that allows the assimilation of statistical informations into chaotic ocean models on longer time scales than the predictability range. The basic underlying assumption is that a larger predictability exists for planetary scales which are isolated by temporal and spatial averaging. The crucial point of the method is the invention of an adjoint to a separate prognostic model for the statistical mean used to calculate the cost function gradients. Coarse resolution versions of eddy resolving models are applied for this purpose. Here we use a $1/3^o$ eddy-permitting forward model in combination with a 1^o backward model. For higher order moments such as sea surface height variance calculated from altimeter data, a closure scheme is required, which is employed by a simple parameterization in analogy to the approach of Green (1970) and Stone (1972). The method is applied for the assimilation of annual SSH variance calculated from TOPEX/POSEIDON and ERS1 in association with climatological data for temperature and salinity from Boyer and Levitus (1997) into an eddy permitting version

continued on page 19

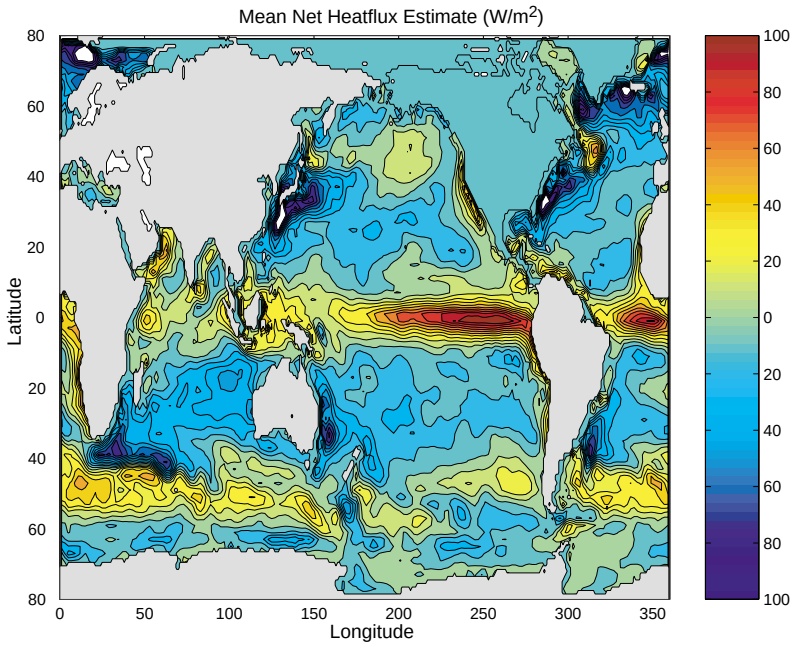

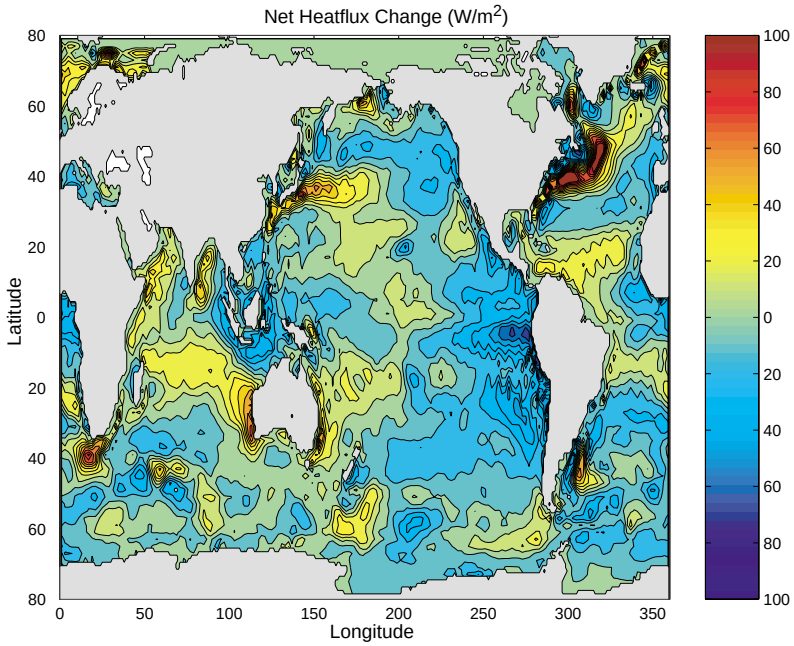

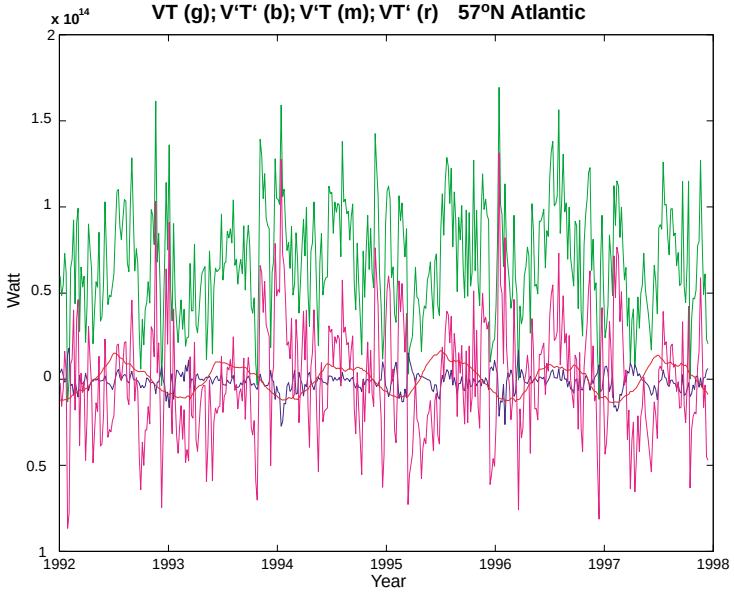

Stammer et al., Ocean state estimation in support of CLIVAR and GODAE, page 3:

Figure 2: The mean net surface heat field as it results from the optimisation is displayed in the upper panel. Its mean change relative to the prior NCEP fields is provided in the middle pannel. All resulting modifications of the net NCEP heat fluxes, which are of the order of 20 Wm^{-2} over large parts of the interior oceans and reach 80 Wm^{-2} along the boundary currents, are consistent with our prior understanding of NCEP heat flux errors.

Bottom pannel: The estimated net fluxes H_q is shown across 25° N in the North Atlantic (green line). It can be decomposed in to a mean and a time varying part

$$H_q(t) = \iint \bar{v}\bar{\theta}\,dzdx + \iint v'\theta'\,dzdx + \iint \bar{\theta}\,v'\,dzdx + \iint \bar{v}\theta'\,dzdx$$

where the bar indicates the time-average. The latter three terms are displayed as blue, magenta and red lines, respectively.

The last term in θ' gains importance towards high latitudes and is responsible for almost all changes on the seasonal cycle in mid and high latitudes. The second and third terms involving v' are somewhat larger but to some extend cancel each other during winter seasons, especially in high latitudes where they are also smaller but in phase during summer time. Towards low latitudes, most of the variability in the meridional heat flux comes from the $v'\bar{\theta}$ term, while the two other terms are very small.

***Guinehut et al., Design of an array of profiling floats in the North Atlantic from Model simulations - preliminary results, page 6**:*

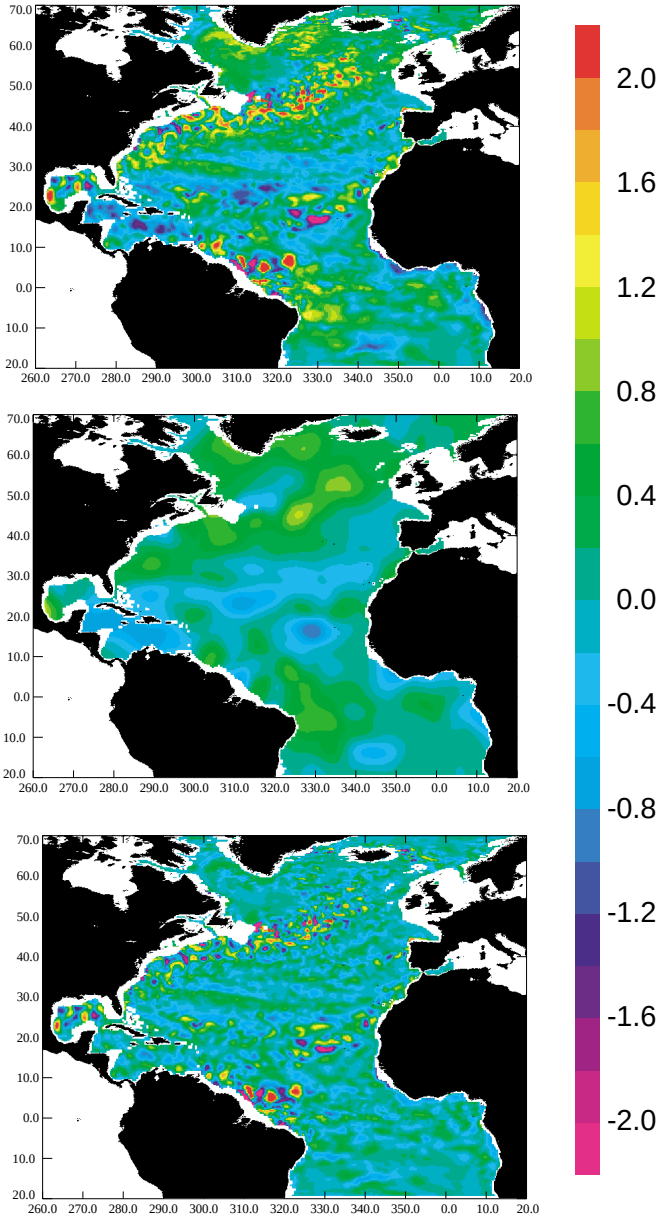

Figure 1: (a) Instantaneous temperature anomalies at 200 m (01/01/89) and corresponding large scale (b) and mesoscale (c) signals (in °C).

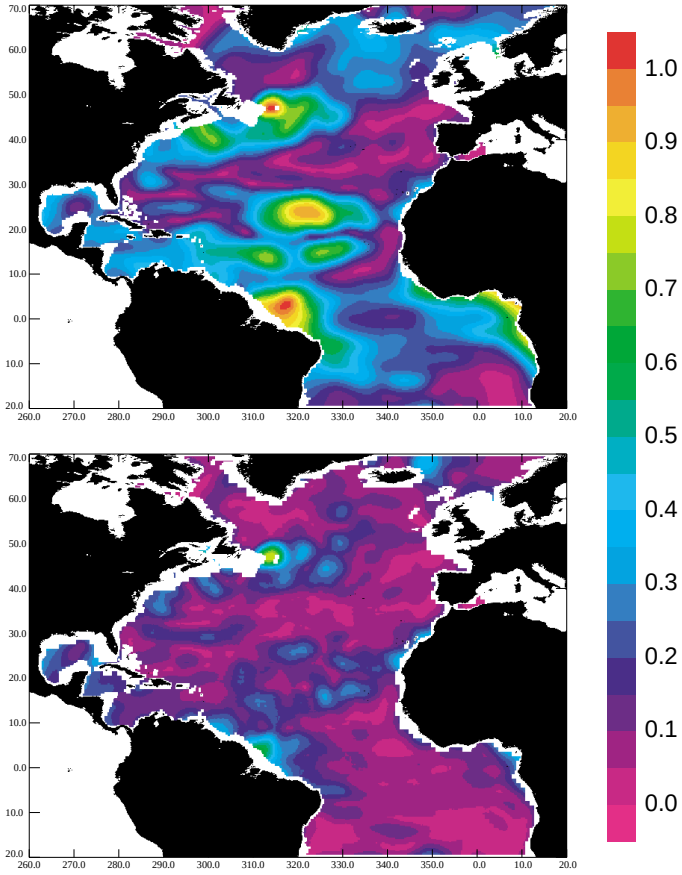

Figure 2: (a) Rms of the monthly means of the large scale signal of temperature anomalies at 200 m and (b) rms of mapping error for the three-degree array (in °C).

Tippnett et al., Impact of temperature error models in a univariate ocean data assimilation system, page 13:

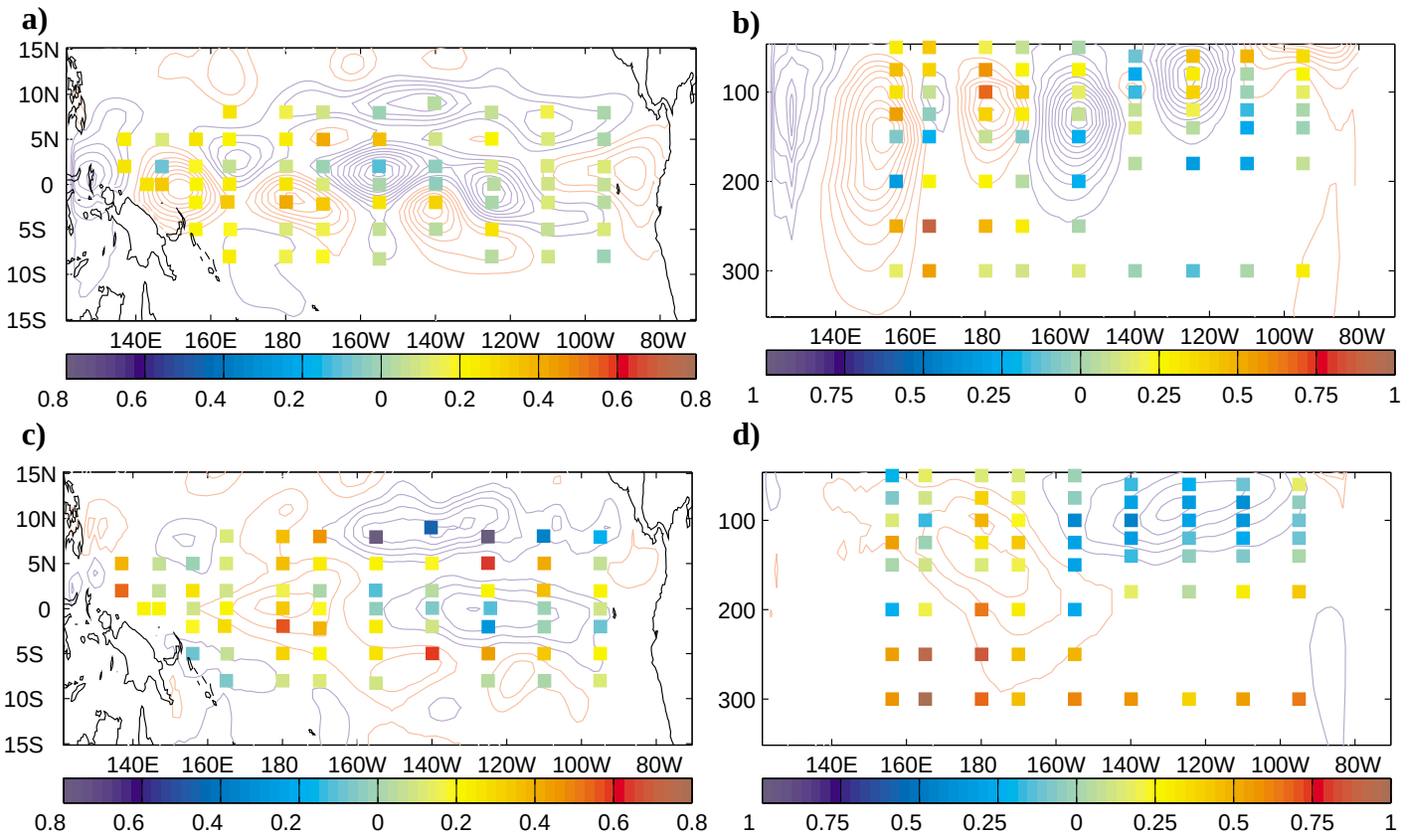

Figure 1(above): Mean temperature corrections (positive (negative) contours are red (blue)) and TAO observations minus analysis (colored squares) (a) vertically averaged (50 - 500m; contour interval of 0.004°C / hour) and (b) along the equator (contour interval of 0.008°C / hour)) for the control case. (c) and (d) as in (a) and (b) but for the reduced space analysis.

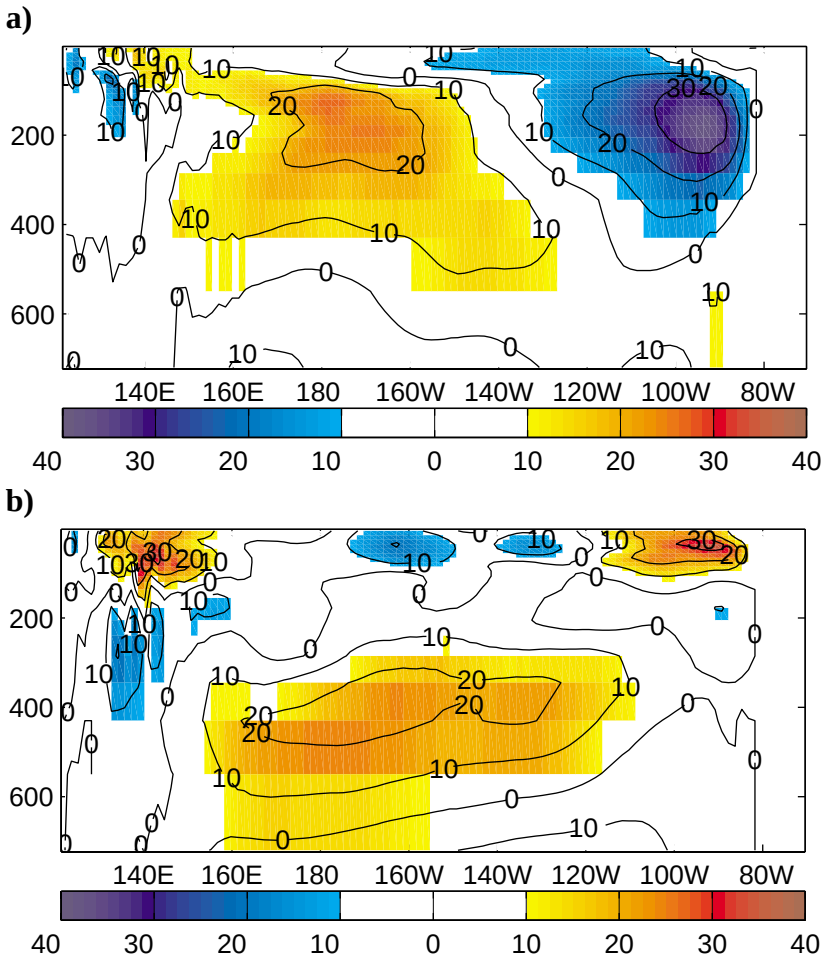

Figure 2: Mean difference in cm/sec of simulation equatorial zonal currents and (a) control analysis and (b) reduced-space analysis.

Wyputta and Grieger, Comparison of ocean forcing fields from PMIP simulations, page 26:

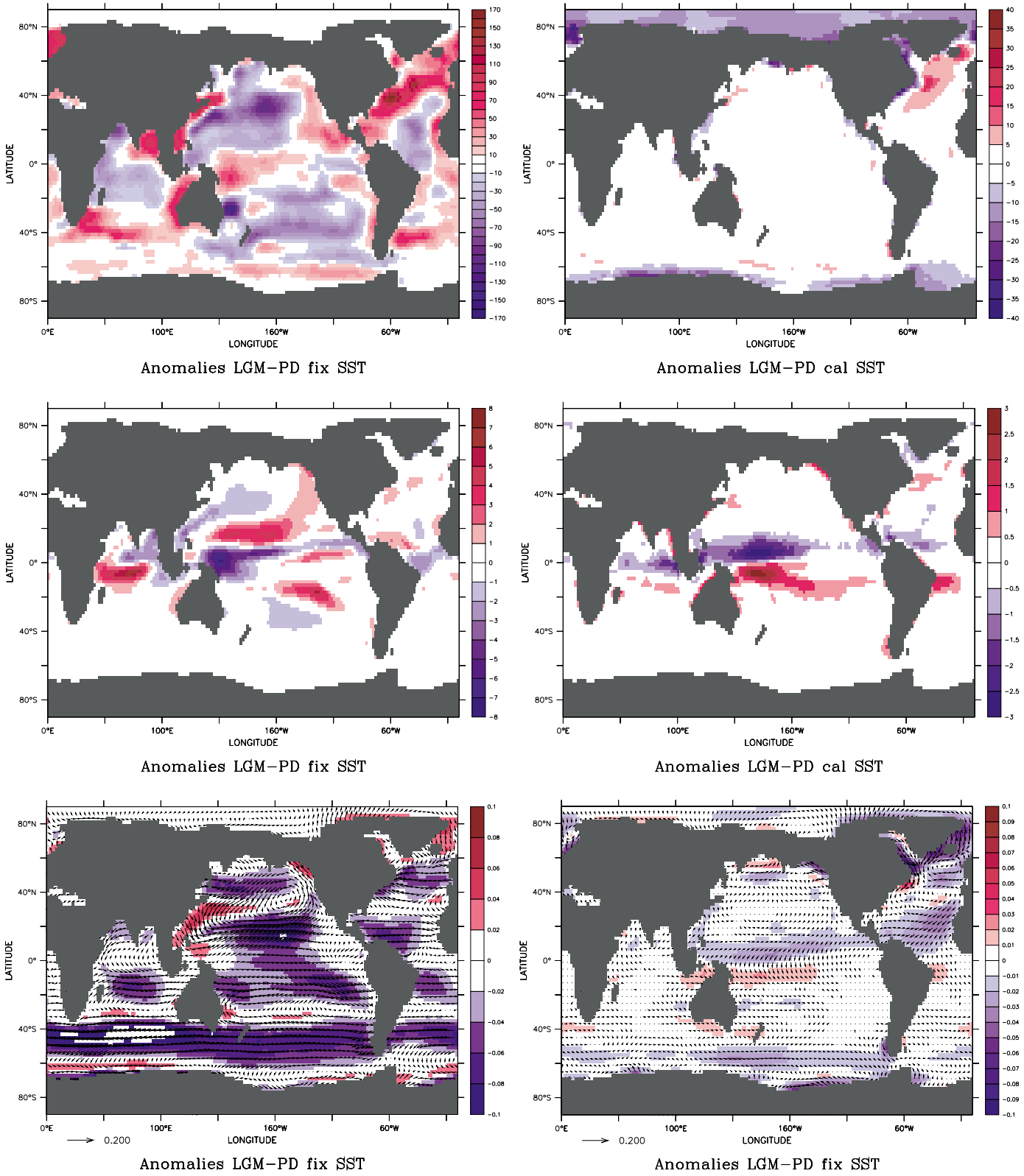

Figure 1:
Top: Anomalies of heat flux as mean of 5 models using fixed SSTs (left), and 4 models using calculated SSTs (right).
Center: Anomalies of fresh water flux as mean of 7 models using fixed SSTs (left), and 6 models using calculated SSTs (right).
Bottom: Anomalies of wind stress as mean of 5 models using fixed SSTs (left), and of 6 models using calculated SSTs (right).

continued from page 14

of the Community Modelling Effort model of the North Atlantic ocean. The intention is to utilize the close correspondence between the position of the main frontal structures and the patterns of high variability as demonstrated by Treguier et al. (1997) to estimate the underlying mean state by assimilating variability.

The forward model is described in Oschlies and Willebrand (1996). The horizontal gridspacing is 1/3° in meridional and 2/5° in zonal direction. It is forced with monthly mean wind stresses of Hellerman and Rosenstein (1983) and the heat flux is formulated according to the linear approximation of Han (1984). Surface fluxes of fresh water are specified by relaxating salinity to the monthly mean values of Levitus (1982). The adjoint is constructed from the modified code of the 1 degree version with aid of the automatic adjoint code compiler TAMC developed by Giering and Kaminski (1998). Initial conditions for temperature and salinity are estimated and mean values of the subsequent year are analysed.

The effect of the parameterization which is based on baroclinic instability theory is to suggest steeper frontal structures at locations where the 1/3° model underestimates variability in proportion to the observations. The locations of the Azores front and the Gulf Stream are clearly visible in the cost function gradient from the first iteration displayed in Figure 1 . The gradient results from the SSH-variance data term alone and it is directly related to the proposed changes of the temperature initial condition. Spatial gradients visible in Figure 1 thus correspond to spatial gradients in the change of the temperature field.

It is found that SSH variance data can introduce complementary informations about the main frontal structures

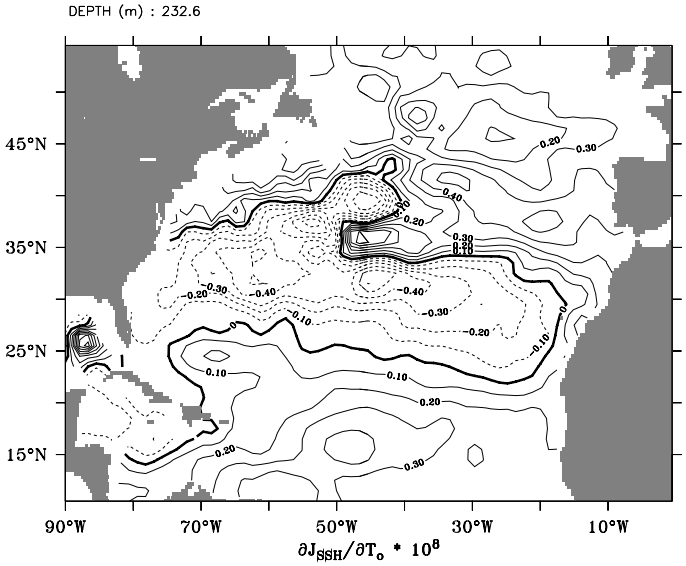

Fig. 1: Horizontal section through the gradient of the cost function part JSSH with respect to the temperature initial condition. The cost function part JSSH measures the difference of the SSH variances between observed and simulated, ci=0.1°C^{-1}; dashed lines negative.

consistent with climatologies since sharp fronts are usually appear too smooth in climatological data. Figure 2 (page 20) demonstrates the close linkage between mean SSH and its variability. The mean front of the control as visible from mean SSH and the associated variability is displaced northward and too weak. The mean SSH is corrected after optimization to almost the same position and strength visible in the data from Singh and Kelly (1997), although the northward turn of the North Atlantic Currrent at 42°W is not captured. According to the physical basis implemented within the closure scheme baroclinic instability is enhanced in connection with the strengthening of the frontal structures. The level of variability is increased to the observed, although the pattern extends slightly further to the north around 55°W and misses the extension at 40°W. Eddy scales remain too large due to still too low resolution.

The resulting annual mean state, though not fully consistent with the assimilated data, is markedly improved in comparison with the reference state. Not surprisingly, after a few years of forward integration without assimilation the state will however return back to the first guess state.

Acknowledgements

The work was supported by the German WOCE through the BMBF under contract number 03 F 0157 A.

References

Boyer, T. P., and S. Levitus, 1997: Objective analyses of temperature and salinity for the world oceanon a 1/4degree grid. *NOAA Atlas NESDIS 11*, U.S. Gov. Printing Office, Washington, D.C.

Giering, R., and T. Kaminski, 1998: Recipes for Adjoint Code Construction. *ACM Trans. on Math. Software*, **24**, 437-474.

Green, J. S. A., 1970: Transfer properties of the large-scale eddies and the general circulation of the atmosphere. *Q. J. R. Meteor. Soc.*, **96**, 157-417.

Han, Y.-J., 1984: A numerical world ocean general circulation model part II. a baroclinic experiment. *Dyn. Atmos. & Oceanogr.*, **8**, 141-172.

Hellerman, S., and M. Rosenstein, 1983: Normal monthly windstress over the world ocean with error estimates. *J. Phys. Oceanogr.*, **13**, 1093-1104.

Levitus, S., 1982: Climatological atlas of the world ocean. *NOAA Tech. Paper*, 173 pp.

Oschlies, A., and J. Willebrand, 1996: Assimilation of Geosat altimeter data into an eddy-resolving primitive equation model of the North Atlantic Ocean. *J. Geophys. Res.*, **101**, 14,175-14,190.

Singh, S., and K. A. Kelly, 1997: Monthly maps of sea surface hight in the North Atlantic and zonal indices for the Gulf Stream using TOPEX/Poseidon altimeter data. *Woods Hole Oceanographic Institution Technical Report*, **WHOI-97-06**, 50pp.

Stone, P. H., 1972: A simplied radiative-dynamical model for the static stability of rotating atmospheres. *J. Atmos. Sci.*, **29**, 405-418.

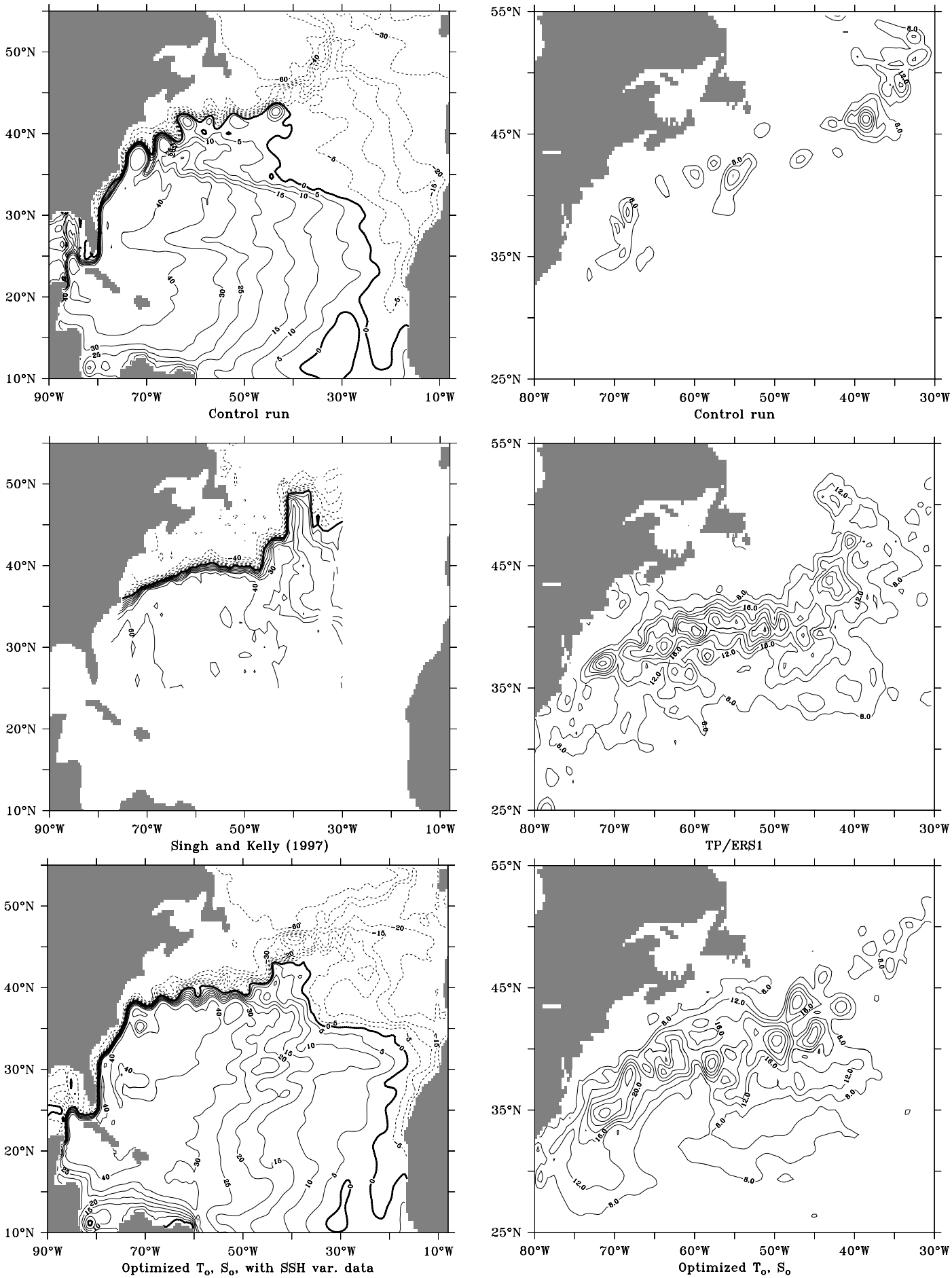

Fig. 2: Mean sea surface height (left) and variance (right) in cm; (upper) control run, (middle) data from observations and (lower) after optimizing initial conditions for temperature and salinity.

The DYNAMO Group, 1997: DYNAMO Dynamics of North Atlantic Models: Simulation and assimilation with high resolution models, Berichte aus dem IFM Kiel Nr. 294.

Treguier, A. M., I. Held, and V. Larichev, 1997: Parametrization of quasigeostrophic eddies in primitive equation ocean models, J. Phys. Oceanogr., 27, 567-580.

STOIC: A study of coupled model climatology and variability in tropical ocean regions

Mike K. Davey, Matt Huddleston
The Met. Office, London Road, Bracknell, UK
mkdavey@meto.gov.uk

Ken R. Sperber
PCMDI, Lawrence Livermore National Laboratory, Livermore, CA, USA, and the model data contributors.

The tropics are regions of strong ocean-atmosphere interaction on seasonal and interannual timescales, so a good representation of observed tropical behaviour is a prime objective for coupled ocean-atmosphere models. As previous assessments focusing on the tropical Pacific have established (Mechoso et al., 1995, Neelin et al., 1992), it has been difficult to develop coupled general circulation models (CGCMs) with the right balance of oceanic and atmospheric processes and interactions in the tropics. Systematic errors in sea surface temperature (SST) were often largest in the equatorial Pacific, and model representations of El Niño Southern Oscillation (ENSO) variability were often weak and/or incorrectly located.

To broaden and update the previous assessments, two companion projects were initiated by the CLIVAR Numerical Experimentation Group 1 (NEG1): the El Niño Simulation Intercomparison Project (ENSIP, organised by Mojib Latif) and the Study of Tropical Oceans In CGCMs (STOIC). (NEG1 subsequently evolved into the CLIVAR Working Group on Seasonal to Interannual Prediction, WGSIP) Monthly SST, surface wind stress and upper ocean vertically averaged temperature (VAT) data from 24 coupled models were collected, along with observational analyses. From the submitted data, annual means, annual cycles and interannual anomalies were calculated for 20-year samples. Of the participating models, 22 are coupled GCMs, of which 14 use no form of flux adjustment in the tropics. The models vary widely in design, components and purpose. Note that the model data were submitted in 1997 and 1998, so the results do not necessarily indicate the performance of current versions. Many of the models have also been assessed collectively as part of the Coupled Model Intercomparison Project (CMIP). Model ENSO behaviour from an atmospheric viewpoint has been described by AchutaRao et al. (2000).

The aim was to compare the various models against observations, to identify common weaknesses and strengths and to provide benchmarks for future models. Results from ENSIP, concentrating on the equatorial Pacific, have been described by Latif et al. (2000), denoted ENSIP2000 henceforth. The STOIC analyses extend beyond the equatorial Pacific, to examine behaviour in all three tropical ocean regions (Atlantic, Indian and Pacific), including inter-ocean relationships. A detailed report on STOIC has been completed, and is available via anonymous ftp at ftp://email.meto.gov.uk/pub/cr/ in the gzipped files mkdavey_stoic_doc.gz (text as Word document) and mhuddleston_stoic_figs_050700_tar.gz (postscript figures). Some of the main annual and interannual features found in the comparisons between models and observations are summarised below. For observations we have used the GISST3 SST dataset from The Met. Office, wind stress from WM-COADS and Southampton Oceanography Centre, and upper ocean temperature from Scripps Institution of Oceanography.

Annual mean SST

The equatorial section for CGCMs with no tropical 'flux adjustment' is shown in Fig. 1 (page 1). The labels indicate the various models: for details see the detailed report or ENSIP2000. (Note: the PAC and ATL sub-labels denote separate submitted datasets. However, only UCLA PAC and UCLA ATL are actually different CGCMs.) In most of the Pacific sector, described in detail in ENSIP2000, it is evident that most models have SST too cool by 2 to 3°C, but the strong central equatorial Pacific east-west SST gradient is by and large correct. Several have substantial warm biases in the east Pacific approaching the South American coast. In the equatorial Atlantic nearly all models have the wrong east-west gradient, with SST commonly too cool in the west and too warm in the east. In the Indian ocean sector most models simulate the SST gradient quite well, often with a cold bias. From meridional SST sections it is also evident that most have a too-prominent equatorial cold trough in the east Pacific and central Atlantic.

Among the 8 CGCMs with 'flux adjustment' (not shown), all but one has SST within +/- 1°C of observations over most of the equatorial region.

Annual mean zonal wind stress

Several common features were evident over the equatorial oceans: the majority of the models have mean easterlies that were too weak in the equatorial Atlantic, and westerlies too weak (easterly in several cases) in the Indian sector. Among CGCMs with no 'flux adjustment', most have easterly wind stress too weak in the central equatorial Pacific but easterly wind stress too strong in the west equatorial Pacific. Among CGCMs with 'flux adjustment' mean zonal wind stresses were generally close to observed values in the equatorial Pacific, with largest differences in the central Pacific, but were often too weak in the Indian and Atlantic sectors.

With regard to the Pacific, the mean equatorial SST errors are quite similar to those found in previous CGCM

comparisons. The wind stress errors are also similar, with too-weak (too-strong) central (west) Pacific easterly wind stress accompanying too-cold SST in most of the 'no-adjustment' group. There is also still a tendency for the cold tongue to be too narrow and too strong. As many of the OGCMs use basically the same mixing and advection schemes as in the Mechoso et al. (1995) CGCM sample, it seems likely that errors in representing upper ocean equatorial mixing and circulation (compounded by ocean-atmosphere interaction and feedbacks) lead to these equatorial biases. The warm bias in the east equatorial Pacific SST is also common to previous CGCM assessments, and here it is also evident in the Atlantic. This is often associated with reductions in stratus cloud in those regions in CGCMs.

Interannual variability

In the equatorial central-east Pacific most models (both with and without flux adjustment) substantially underestimated the observed SST variability levels, while many had excess variability in the west Pacific. This was a symptom of a tendency to misplace maximum variability too far west. The majority of models also underestimated SST variability in the Atlantic sector, but matched observed levels in the Indian ocean. With regard to zonal wind stress, most models also substantially underestimated central equatorial Pacific variability, many underestimated variability in the Indian region, but most were comparable to observed levels in the Atlantic sector.

The Pacific results are illustrated in Fig. 2 by a scatterplot of SST standard deviations in the Niño-3 region (5°N-5°S, 150°W-90°W)) against zonal wind stress standard deviation in a central equatorial Pacific region (5°N-5°S,165°E-225°E). Although allowance must be made for the effect of the limited sample sizes, regions selected, and multi-decadal fluctuations in activity, is is evident that few of the models approach observed levels of interannual variability. As expected in a region of strong ocean-atmosphere coupling, wind stress variability tends to increase with SST variability. The lack of model wind stress variability is often more severe than the shortfall in SST variability.

With regard to interannual variability, the 'no-adjustment' group tended to perform better than the 'adjusted' group. Part of the explanation for this difference is likely to be that the 'no-adjustment' models generally had higher resolution than the 'adjusted' models, particularly in the near-equatorial ocean regions. Note also that simulation of tropical variability was not a primary aim for several of the models.

Interannual correlations between SST' and Niño-3 SST'

Observations reveal a distinctive horseshoe pattern of negative correlations in the tropical Pacific, but only a few models could reproduce this feature. Most incorrectly had positive correlations in the west equatorial Pacific, which is largely a consequence of having the maximum

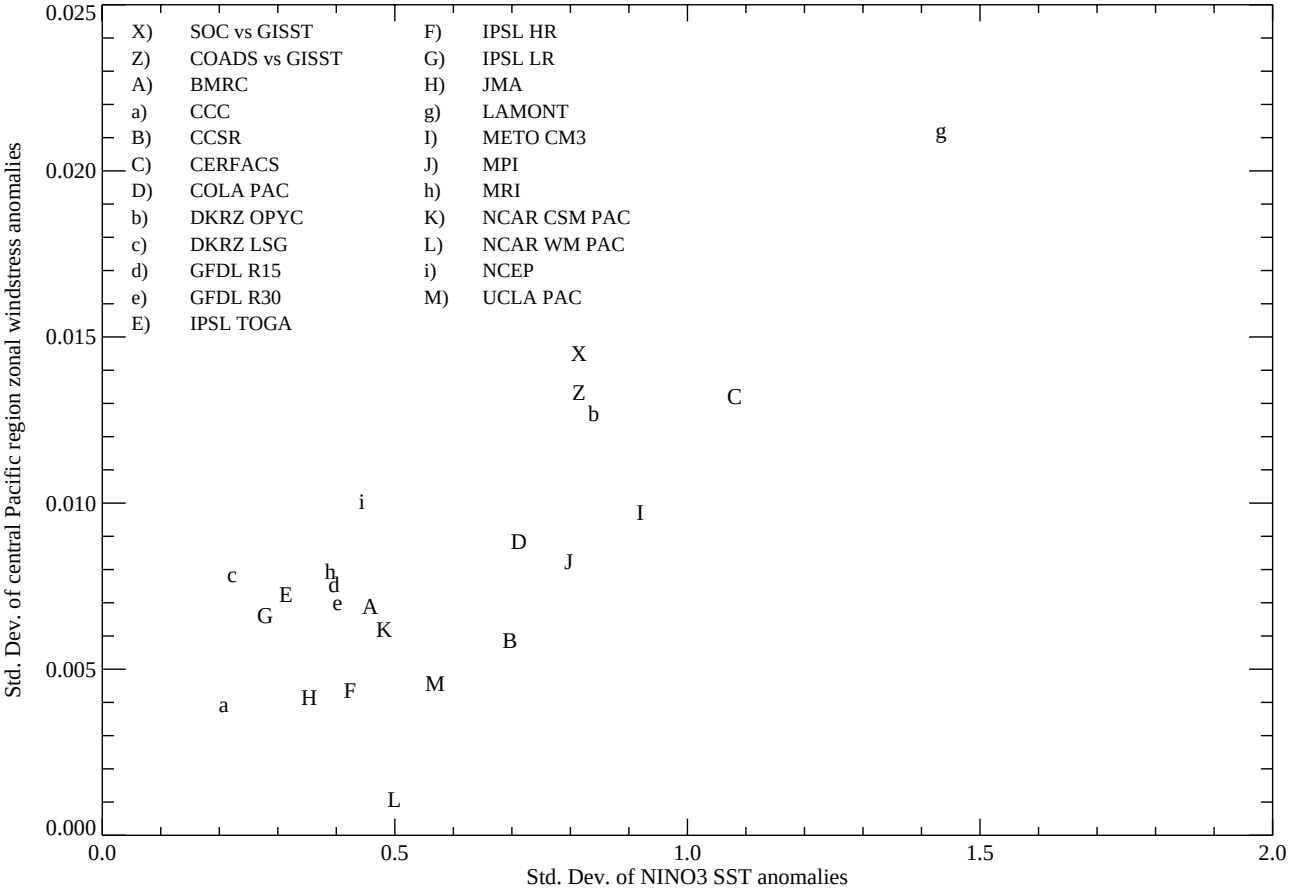

Fig. 2: Scatterplot of interannual standard deviations of SST in region Niño-3 and zonal wind stress in the central equatorial Pacific (5N-5S,165E-225E). Lower case symbols indicate models with flux adjustment, while X and Z indicate observed values.

SST variability misplaced to the west. Most models could not reproduce the observed extension of substantial positive correlations along the north American coast from the east equatorial Pacific - this failure may reflect the relatively low off-equatorial spatial resolutions of the oceanic components.

Most models underestimated the observed positive correlation of Indian ocean SST′ with Pacific Niño-3 SST′, and only a few (all 'no-adjustment') could capture the robust observed lag relationship with the central Indian ocean region, which has a positive correlation peak with the Pacific leading by several months.

Nearly all models did have a positive correlation between Niño-3 and some part of the north tropical Atlantic, as observed, and several had a lead-lag relation resembling that observed.

ENSO wind stress composites

Although it was difficult to find robust wind signals via correlations, the use of composites proved very effective. Most models performed quite well in terms of reproducing the sign of observed ENSO composite wind stress features in the tropics, though magnitude varied widely.

The main problems to fix

The equatorial oceans are still a major problem area for coupled models. In the 'no-adjustment' group the drift to too-cold equatorial Pacific SST remains the main climatological error, but there are also substantial biases in the other oceans.

Surface wind stress is a major common problem with regard to the seasonal cycle in all ocean sectors and levels of variability in the Pacific. As the errors also arise for models in the 'adjusted' group, which generally have an SST climatology kept close to that observed, these errors cannot simply be attributed to coupled drift.

Are 20-year samples adequate?

The 20-year samples used for STOIC and ENSIP seem to be adequate for assessing annual mean and seasonal cycle behaviour; particularly as the model biases are large and gross errors are readily apparent. The samples also seem adequate for assessing the dominant features in patterns of variability, and for determining gross errors in levels of variability. However, the reliability of quantitative results is questionable, as the statistics of both models and observations vary on decadal and longer timescales.

For future such comparisons, longer (100-year?) model samples would be preferable to increase the reliability of assessments of interannual variability.

Acknowledgement

K.R. Sperber was supported under the auspices of the US Department of Energy Environmental Sciences Division at the Lawrence Livermore National Laboratory under Contract W-7405-ENG-48.

References:

AchutaRao, K., K.R. Sperber, and the CMIP modelling groups, 2000: El Niño Southern Oscillation in coupled GCMs. In preparation.

Latif, M., K.R. Sperber, et al., 2000: ENSIP - The El Niño simulation intercomparison project. *Climate Dynamics*, submitted.

Mechoso, C.R., A.W. Robertson, N. Barth, M.K. Davey, P. Delecluse, P.R. Gent, S. Ineson, B. Kirtman, M. Latif, H. Le Treut, T. Nagai, J.D. Neelin, S.G.H. Philander, J. Polcher, P. S. Schopf, T. Stockdale, M.J. Suarez, L. Terray, O. Thual, and J.J. Tribbia, 1995: The seasonal cycle over the tropical Pacific in general circulation models. *Mon. Wea. Rev.*, **123**, 2825-2838.

Neelin, D., M. Latif, A.F. Allaart, M.A. Cane, U. Cubasch, W. L. Gates, P.R. Gent, M. Ghil, J. Meehl, J.M. Oberhuber, S.G.H. Philander, P.S. Schopf, K.R. Sperber, A. Sterl, T. Tokioka, J. Tribbia, and S.E. Zebiak, 1992. Tropical air-sea interaction in general circulation models. *Climate Dynamics*, **7**, 73-104.

The ocean heat transport and meridional overturning near 25°N in the Atlantic in the CMIP models

Yanli Jia
Southampton Oceanography Centre, Southampton, UK
Yanli.Jia@soc.soton.ac.uk

1. Introduction

The models considered in this article are participants of the Coupled Model Intercomparison Project (CMIP). CMIP examined climate variability and predictability as simulated by the models, and compared the model output with observations where available (Covey and Meehl, 1997). In the first phase (CMIP1), the performance of the models in producing the mean climate was examined using model output from "control experiments", in which the external forcing terms such as atmospheric CO_2 concentration and solar luminosity are held constant. For the second phase of the project (CMIP2), model responses to an idealised scenario of anthropogenic climate forcing (a 1% per year increase in atmospheric carbon dioxide) are examined. Parallel "control experiments" are also available. Analysis of the model output is done partly in the form of diagnostic subprojects. This article reports some of the results from one such subproject that concerns the ocean components of the coupled models. The focus is on the ocean heat transport.

Recent advances in both atmospheric and ocean general circulation models have resulted in much improved

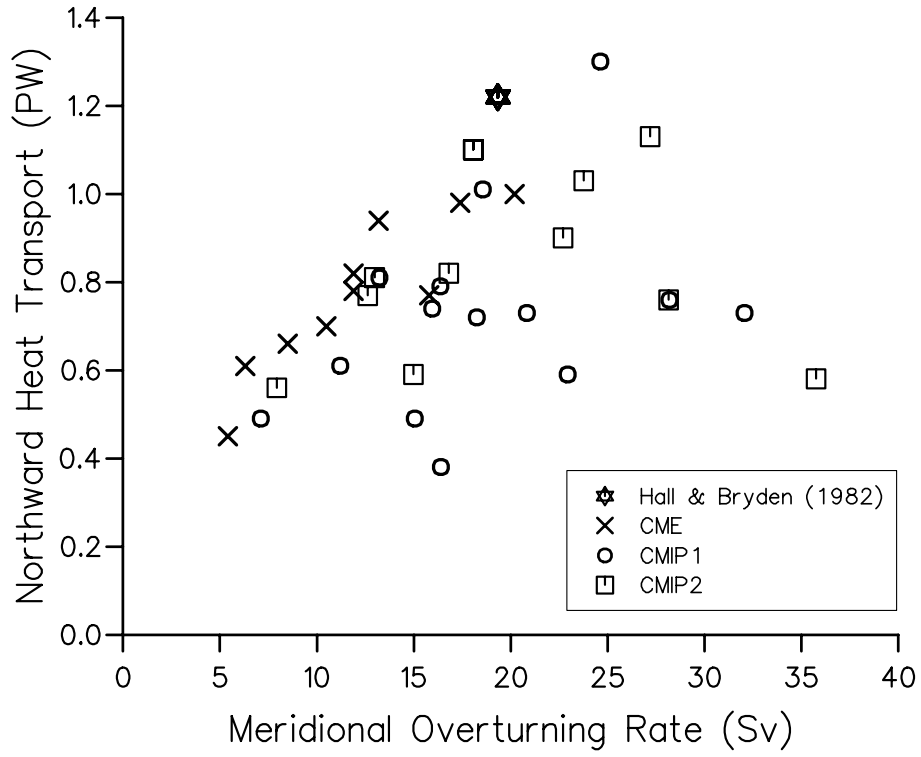

Fig. 1. The total northward ocean heat transport is displayed as a function of the strength of the overturning circulation near 25°N in the Atlantic. The star is for the observational estimate based on Hall and Bryden (1982), the crosses are for the CME experiments from Böning et al. (1996), the circles are for the CMIP1 models, and the boxes are for the CMIP2 models.

coupled models that are capable of producing stable SST without the need for flux corrections (e.g. Boville and Gent, 1998; Gordon et al., 2000). This success is believed to be a result of the compatibility in the poleward heat transports by the atmosphere and the ocean components. However, more often the ocean heat transport computed from an ocean model or the ocean component of a coupled model is lower than that derived from observed atmospheric fluxes or implied by atmospheric models. In a coupled ocean-atmosphere general circulation model, such a discrepancy will lead to a climate drift that introduces great uncertainties to the understanding of anthropogenic climate change.

Based on direct oceanographic measurements, Bryden (1993) pointed out the different mechanisms of ocean heat transport in the North Atlantic and the North Pacific oceans, and emphasised the ultimate dependence of ocean heat transport on ocean circulation. In the North Atlantic, the meridional heat transport is achieved through the meridional overturning circulation driven by thermohaline circulation, while in the North Pacific the meridional heat transport is accomplished by the horizontal circulation driven by wind forcing. In this article, the ocean heat transport across 25°N in the Atlantic from the "control experiments" of CMIP1 and CMIP2 is compared with estimates from oceanographic measurements, and its correlation to the oceanic structure and ocean circulation is investigated.

2. Model results

Hall and Bryden (1982) estimated the total ocean heat transport across 25°N in the Atlantic to be 1.22 PW (PW=10^{15}W) northward from direct oceanographic measurements (1957 IGY section). This estimate is supported by several other calculations (inverse or direct) based on measurements made in 1981 (Roemmich and Wunsch, 1985) and 1992 (Lavín et al., 1998). The northward heat transport is due entirely to a deep vertical-meridional circulation cell, with northward flowing warm surface waters in the form of a western boundary current (the Gulf Stream) and southward flowing cold deep waters (the North Atlantic Deep Water). The contribution from the horizontal circulation is negligible (0.06 PW southward (Bryden 1993)). The strength of the meridional overturning circulation at 25°N is estimated to be 19.33 Sv (Sv = 10^6m^{3}s^{-1}) from Table 5 of Hall and Bryden (1982).

The total heat transport and the strength of the meridional overturning circulation near 25°N are extracted from fourteen CMIP1 models and eleven CMIP2 models (some of the CMIP2 models are participants of CMIP1 as well) and are displayed in Fig. 1 together with the estimates from Hall and Bryden (1982). We see that all but one of the models underestimate the total heat transport at this latitude.

Böning et al. (1996) derived a near linear relation between the upper cell overturning rate and the total heat transport at 25°N from a set of experiments (also displayed in Fig. 1) using the ocean model developed under the Community Modelling Effort (CME). It is suggested that for every 2 Sv gain in the overturning rate, the heat transport across 25°N increases by approximately 0.1 PW. Such a correlation is also found in several other ocean only models (e.g. the three DYNAMO ocean models, see DYNAMO Group (1997)).

As shown in Fig. 1, a large number of the CMIP coupled models, however, do not follow the linear trend, with the heat transport much lower than the correlation would suggest. This result is not unexpected. Assuming that the contribution from the horizontal gyre circulation is negli-

gible, the heat transport depends not only on the strength of the overturning rate but also the temperature difference between the upper and lower branches of the overturning cell. In the case of the ocean only models, a near linear correlation indicates that the temperature difference is very similar among the models. This is perhaps because the integrations are usually for a small number of centuries and the model oceans do not drift very far from their initial conditions. To demonstrate this, diagnostic calculations are performed with model outputs from one of the DYNAMO models, the MICOM model (a layer model at 1/3° resolution). The total integration length is for 20 years and the final 5 years are used for the diagnostic calculation. At 25°N, the overturning rate is 19.07 Sv, the total heat transport is 1.16 PW (the gyre contribution is 0.001 PW southward). The average temperatures (the zonal mean temperature weighted by the zonal mean volume transport) of the upper and lower branches of the meridional cell are 17.70°C and 2.86°C respectively, yielding a temperature difference of 14.84°C.

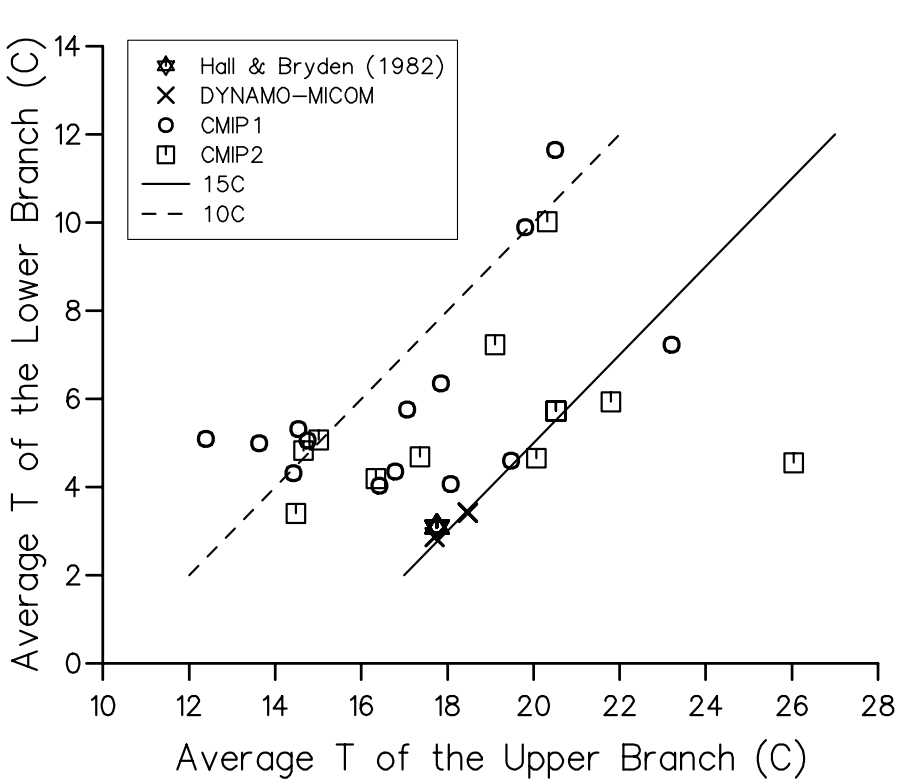

Fig. 2. The average temperatures (weighted by the volume transport) of the upper and lower branches of the overturning cell near 25° N in the Atlantic. The symbols are the same as for in Fig. 1 except that the crosses are for the DYNAMO experiments. The solid line indicates a temperature difference of 15°C between the upper and lower branches, and the dashed line is for 10°C.

The same model was integrated for 30 years at a lower resolution (4/3°). At 25°N, it produced an overturning rate of 15.93 Sv, a total heat transport of 0.95 PW (the gyre contribution is 0.03 southward). The average temperatures of the upper and lower overturning branches are 18.47°C and 3.42°C respectively, yielding a temperature difference of 15.05°C.

The lower heat transport obtained from the coarse resolution experiment, therefore, is mostly due to the lower overturning rate (resulting from weaker production of NADW in the high latitudes) as the temperature difference is very similar to that in the higher resolution experiment. The observational estimates of the average temperatures of the upper and lower branches are obtained by making use of the information in Table 5 of Hall and Bryden (1982). The results are 17.76°C for the upper branch, 3.08°C for the lower branch, and a temperature difference of 14.68°C.

At a temperature difference of 15°C (as suggested by the observational estimate and model results from the DYNAMO MICOM experiments), the heat transport would increase at a rate of 0.12 PW for every 2 Sv increase in the overturning strength. This rate is consistent with the linear trend derived by Böning et al. (1996). At a smaller temperature difference of 10°C, it reduces to 0.08 PW per 2 Sv. The average temperatures are also computed for the CMIP models and are displayed in Fig. 2. We see that a large number of the models have the temperature difference below 15°C, most fall between 15°C (the solid line) and 10°C (the dashed line), with a few outside this range. The coupling of a small temperature difference and a weak overturning strength is the primary cause of a low heat transport for most of the coupled models. Yet for some other models, the overturning strength is far higher than the observational estimate but the heat transport is still low. Further investigations reveal that the contribution from the horizontal gyre circulation in some of the models is not negligible but significantly southward (greater than 0.3 PW) thus further reducing the magnitude of the total northward heat transport.

Fig. 2 also shows that all the models have a too warm deep ocean, some are only slightly but others are far warmer than the observational estimate. This is an indication that certain high latitude processes (e.g. deep convection, overflows and diapycnic mixing) are not properly represented by these models, a problem that is already recognised by ocean modellers (see WOCE (1999)). We also see from Figs. 1 and 2 that the strength of the overturning circulation and the average temperature of the upper branch vary over wide ranges among the models, a reflection that there is much uncertainty in the physical processes that determine these two elements.

To conclude, there are considerable challenges in achieving the correct ocean heat transport in climate models. They involve improved understanding of many physical processes that determine various aspects of ocean circulation and oceanic structure. The synthesis of the hydrographic measurements made during WOCE should help in this endeavour.

Acknowledgments

I would like to thank David Webb for introducing me to CMIP, Curt Covey for many correspondences with regard to data availability and transfer, Steve Lambert and Emmanuelle Cohen-Solal for compiling the CMIP1 model output used in this study, and all the participating modelling groups for providing their model output.

References

Böning, C.W., F.O. Bryan, W.R. Holland, and R. Döscher, 1996: Deep-water formation and meridional overturning in a high-resolution model of the North Atlantic. *J. Phys. Oceanogr.*, **26**, 1142-1164.

Boville, B.A., and P.R. Gent, 1998: The NCAR Climate Systems Model, Version One. *J. Climate*, **11**, 1455-1471.

Bryden, H.L., 1993: Ocean heat transport across 24°N latitude. In: Interaction Between Global Climate Subsystems, The legacy of Hann (G. A. McBean, and M. Hantel, eds.). *Geophysical Monographs*, **75**, 65-75.

Covey, C., and J. Meehl, 1997: The Coupled Model Intercomparison Project (CMIP). CLIVAR Exchanges, **Vol 2**, No. 3/4, 5-6.

DYNAMO Group, 1997: *Dynamics of North Atlantic Models: Simulation and Assimilation with High Resolution Models.* Berichte aus dem Institut für Meereskunde an der Christian-Albrechts-Universität, Kiel, Nr. 294, 334 pp.

Gordon, C., C. Cooper, C. A. Senior, H. Banks, J. M. Gregory, T. C. Johns, J. F. B. Mitchell, and R. A. Wood, 2000: The simulation of SST, sea ice extents and ocean heat transports in a version of the Hadley Centre coupled model without flux adjustments. *Climate Dynamics*, **16**, 147-168.

Hall, M. M., and H.L. Bryden, 1982: Direct estimates and mechanisms of ocean heat transport. *Deep-Sea Res.*, **29**, 339-359.

Lavín, A., H.L. Bryden, and G. Parrilla, 1998: Meridional transport and heat flux variations in the subtropical North Atlantic. *The Global and Ocean System*, **6**, 269-293.

Roemmich, D., and C. Wunsch, 1985: Two transatlantic sections: meridional circulation and heat flux in the subtropical North Atlantic Ocean. *Deep-Sea Res.*, **32**, 619-664.

WOCE International Project Office, 1999: Report of the WOCE/CLIVAR Workshop on Ocean Modelling for Climate Studies, NCAR, August 1998. WOCE Report No. 165/99, ICPO Publication Series No. 28, 56pp.

Comparison of ocean forcing fields from PMIP simulations

Ulrike Wyputta, and Björn Grieger
Department of Geosciences, University of Bremen, Bremen, Germany
bgri@drulli.palmod.uni-bremen.de

Introduction

The Paleoclimate Modelling Intercomparison Project (PMIP, Joussaume and Taylor, 1995) investigates the physical mechanisms of climate change and the sensitivity of climate models to different parameterisation schemes. 20 atmospheric general circulation models (AGCM) from 9 countries participate in PMIP. With these models, simulations of the atmospheric circulation at two time slices were performed: 6000 years BP, the Holocene Climatic Optimum, when summer insolation was enhanced in the Northern Hemisphere, and 21000 years BP, corresponding to the Last Glacial Maximum (LGM) (e.g. Lorenz et al., 1996). The boundary conditions used for these simulations were agreed upon among the PMIP contractors. Control runs simulating the present atmospheric circulation are also available for each model. The paleoclimate simulations of the different models were compared in order to determine why the results agree in some aspects and differ in others. The paleoclimatic intercomparisons will lead to an improvement of the models' parameterisations for a better simulation of the physical mechanisms, a reduction in the uncertainty of current estimates of climate sensitivity, a determination of the spatial distribution of paleoclimatic changes that are consistent with the prescribed boundary conditions and a set of boundary conditions which can be used to drive models of the other components of the paleoclimate system.

An important component of the climate system is the ocean. To run an ocean model, heat flux, fresh water flux, and the zonal and meridional components of the wind stress are needed. Instead of being prescribed directly, the former two boundary conditions can alternatively be chosen to force the model to given sea surface temperatures and salinities, respectively (Newtonian forcing). For present day (PD), these boundary conditions are available from observational data. For other time slices the data base is very sparse and complete global fields are mostly not available from proxy data. In these cases, a possibility is to use the results of AGCMs. Within PMIP, the needed data are available from 11 different AGCMs (cf. Tab. 1) for PD and LGM. Some of them were run with fixed sea surface temperatures (SSTs) and others with calculated SSTs based on modern ocean heat transport. After interpolating the ocean forcing fields of each model onto the same 2x2 degree grid, mean fields and standard deviations of each quantity are calculated point by point to obtain the regions where the output of the models agrees best and where the largest differences occur. Additionally, an EOF analysis is performed to investigate if and how the model results are related to each other.

Global Fields: Heat Flux

The global fields of heat flux exhibit the same structure for PD and LGM. A transport of heat from the atmosphere into the ocean occurs in the equatorial region and in the upwelling areas of the ocean (west coast of South America and Africa). A heat flux out of the ocean shows up in the regions of the Golf Stream and Kuroshio Current. While for the simulations with fixed SSTs the heat flux is in the range of -170 to 170 W/m^2, for models using calculated SSTs the heat flux falls between -110 and 110 W/m^2.

The most prominent difference between LGM and PD is a considerable heat flux reduction in the Gulf Stream region (Fig. 1, top, page 18). The reduced outward flux east of Greenland is caused by the specified CLIMAP ice distribution for the LGM which covers this region. The reduced flux in the North Atlantic Current region is due to much lower ocean temperatures. In the Pacific changes for models using calculated SSTs are neglectible. For models using fixed SSTs the main changes in the Pacific are a strongly increased heat flux out of the ocean in the Kuroshio Current region and east of Australia and a slightly increased outward flux in the central North and South Pacific. These changes are primarily due to increased SST in the corresponding regions. Higher wind speeds in the Kuroshio Current region account for some of the increased heat flux there.

Local standard deviations represent the differences between the model outputs. The largest differences between models using fixed SSTs are found over the upwelling regions and the areas of the Golf Stream and Kuroshio Current and also in the North Pacific. The global root-mean-square (RMS) value of the local standard deviations is slightly increased for the LGM compared with the PD runs, cf. Tab. 2. This indicates that the model results differ more for the LGM than for PD which may be due to the fact that the models are to some extend tuned to present climate conditions.

For models using calculated SSTs the standard deviations are in the same range for both time slices. For models using fixed SSTs the largest variations among the models occur in the North Pacific and North Atlantic, while considerable differences are also found in the upwelling regions of the oceans. For models using calculated SSTs the variances among the models are larger than the differences between the two time slices.

Fresh Water Flux

For the simulations with calculated SST the global mean field of annual fresh water flux exhibit the same pattern for PD and LGM. The largest values are found in the region of the Inner Tropical Convergence Zone (ITCZ). In the subtropical regions the fresh water flux is negative, i.e. evaporation exceeds precipitation. In high latitudes the fresh water flux is positive but less than in the tropics. Compared to the annual mean field of all models using fixed SSTs, the mean fresh water flux from experiments with calculated SSTs is slightly decreased.

The anomalies between LGM and PD are much smaller for models using computed SSTs (Fig. 1, centre). As for the experiments with fixed SSTs, the largest differences between both time slices occur in the central Western Pacific. Because the ITCZ resides in the same region, the positive anomalies are due to an intensification of fresh water flux in the equatorial region and the negative anomalies are due to a weakening at 10°S in the western Pacific.

	Heat Flux				**Fresh Water Flux**				**Wind Stress**			
	PD		LGM		PD		LGM		PD		LGM	
	fix	*cal*	*fix*	*cal*	*fix*	*cal*	*fix*	*cal*	*fix*	*cal*	*fix*	*cal*
CCM 1						x		x		x		x
CCSR 1	x		x		x		x		x		x	
ECHAM 3	x		x		x		x		x		x	
GENESIS 1										x		x
GENESIS 2	x	x	x	x	x	x	x	x	x	x	x	x
GFDL		x		x		x		x		x		x
LSCELMD 4	x	x	x	x	x	x	x	x				
LSCELMD 5	x		x		x		x					
MRI 2					x		x		x		x	
UGAMP					x	x	x	x	x	x	x	x
UKMO		x		x		x		x		x		x

Tab. 1: Models and output used for these investigations

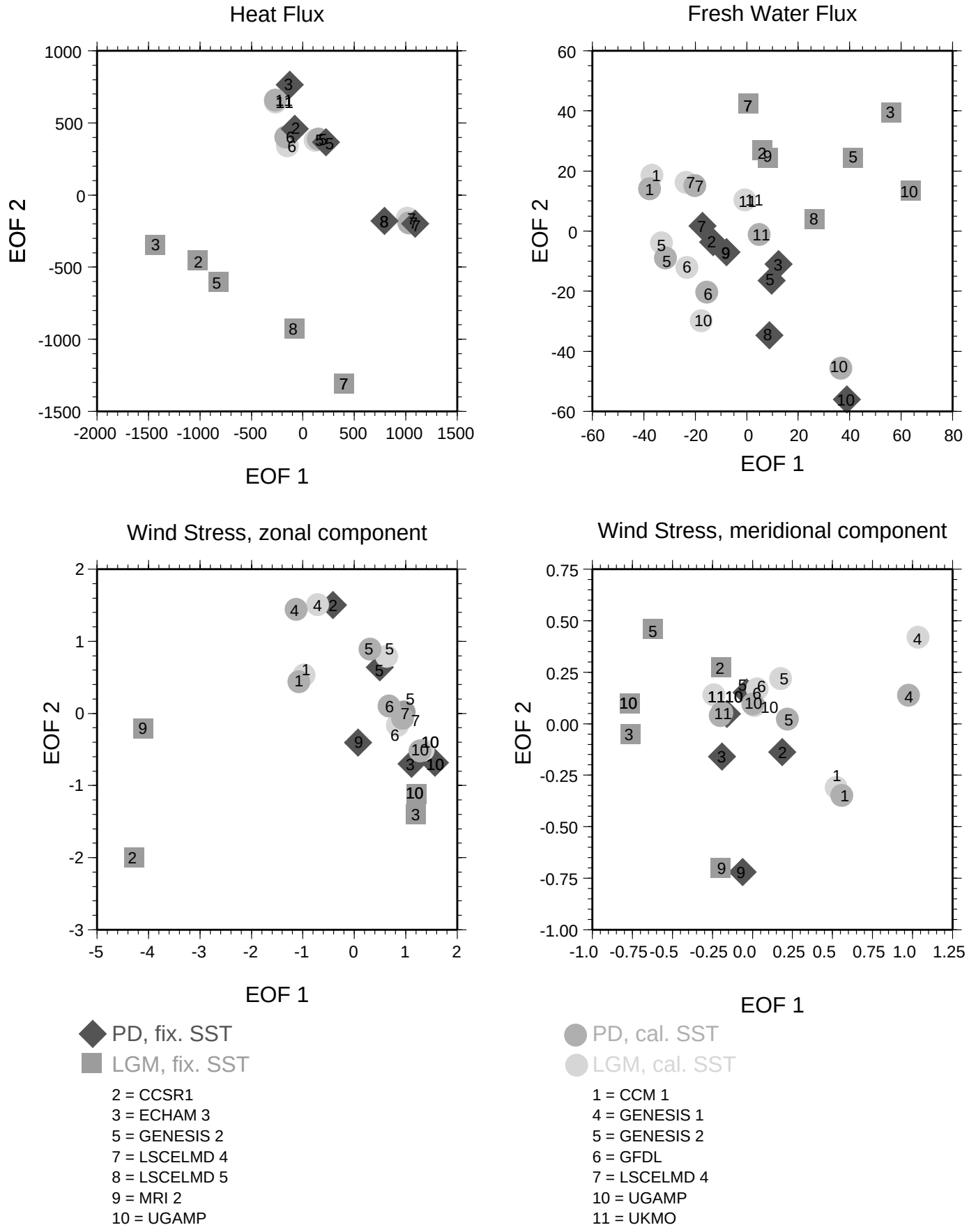

Fig. 2: EOF analysis results for heat flux (top left, fresh water flux (top right), zonal (bottom left), and meridional (bottom right) component of wind stress. The explained variances are 62% for heat flux, 46% for fresh water flux, 88% for zonal, and 53% for meridional wind stress component.

Also for models using fixed SSTs the results exhibit almost the same pattern for the LGM and for PD. The largest anomalies are found over the tropical oceans, where a northward migration of the ITCZ during the LGM corresponds to strong negative values at 20°N in the Pacific and to strong positive values at the equator.

The best agreement among the models for both time slices occur in the mid and high latitudes. With the exception of only small regions, the local standard deviations are between 0 and 1 mm/day. The largest differences among the models are found in the equatorial and tropical regions, where the largest values of fresh water flux occur. For the LGM the area of the worst agreement among the models is extended up to 40°N and 40°S due to the movement of the ITCZ. As for the surface heat flux for models using fixed SSTs, the variances among the models are slightly increased for the LGM and smaller than the differences between the two time slices.

As for surface heat flux, the anomalies between both time slices for models using calculated SSTs are smaller compared to the variances among the models. For simulations using fixed SSTs, the variances among the models are smaller than the anomalies between the time slices (cf. Tab. 2).

Wind Stress

For simulations using calculated SSTs the wind stress anomalies between LGM and PD are only small (Fig. 1, bottom left). Larger differences occur in the equatorial region, in the area of the Antarctic Circumpolar Current (ACC) and in the North Atlantic. Differences among the models are largest in the region of the ACC both for PD and LGM. Even in the global RMS these differences are larger than the anomalies between the time slices.

For models using fixed SSTs the anomalies between LGM and PD are stronger compared to models using calculated SSTs. Again, the anomalies are mainly negative, especially in the Pacific, due to warmer CLIMAP SSTs. Compared to PD the differences among the models are larger for LGM, mainly in the region of the ACC.

EOF Analysis

The EOF analysis was performed separately for heat flux, fresh water flux, and zonal and meridional component of the wind stress. For each of these quantities, the resultant annual mean fields of all models for both time slices are incorporated in the analysis, where only the ocean regions are considered. Each point in the diagrams of Fig. 2 denotes the position of a model resultant field in the space spanned up by the first two principal components. Neglecting higher order components, the distance between two points represents the RMS difference between the corresponding model fields.

Fixed SST

Considering heat and fresh water flux, the models using fixed SSTs are clearly divided into two groups, one containing the experiments for PD (rhomus) and the other containing those for LGM (squares, Fig. 2, top left and right). It can be noticed that the scatter among the models is increased for the latter. This is also implied by the RMS errors of the standard deviations for PD and LGM given in Tab. 2. This behaviour may be due to the fact that the models are to some extend tuned to the present climate and so the variances among the models increase for other time slices. The model scatter within a time slice is of the same order of magnitude than the mean distance between LGM and PD. For all models the anomaly patterns between PD and LGM are more similar than the resultant fields themselves, which is implied by the fact that the vectors connecting PD and LGM results for each model scatter less that the points within a time slice.

For the components of the wind stress from simulations using fixed SSTs no clear distinction between PD and LGM shows up (Fig. 2, bottom left and right). As for heat and fresh water flux, the differences between the LGM simulations are larger compared to PD simulations.

Tab. 2: Model variances

	Mean value		RMS dev.		RMS
Fixed SST	PD	LGM	PD	LGM	**anomalies**
Heat flux (W/m^2)	7.7	4.1	25.3	30.0	35.5
Fresh water flux (mm/day)	-0.41	-0.41	1.2	1.3	1.43
Wind stress (N/m^2)	0.059	0.033	0.038	0.081	0.042
Calculated SST					
Heat flux (W/m^2)	3.9	3.9	26.3	26.2	3.9
Fresh water flux (mm/day)	-0.38	-0.45	1.32	1.31	0.55
Wind stress (N/m^2)	0.059	0.056	0.039	0.040	0.012

For the zonal component this is mainly due to two outliers, which caused the large RMS value in Tab. 2. Generally, for models using fixed SSTs the differences between both time slices are larger than or of the same order of magnitude as the differences among the models for each time slice.

Calculated SST

The changes of heat and fresh water flux and the components of wind stress from PD to LGM are very small for models using calculated SSTs. However, the variances among the models are of the same order of magnitude as those among models using fixed SSTs, thus for models with calculated SSTs no systematic differences between the two time slices can be noticed. The anomaly vectors connecting PD and LGM result of each model point in different directions. As can be noticed in Tab. 2, the differences between the models are larger than the anomalies between the time slices.

For models with calculated SSTs no systematic differences between the two time slices can be seen. The anomaly patterns point into different directions. As can be noticed in Tab. 2, differences among the models are larger than anomalies between time slices.

Summary

The main conclusions for heat flux, fresh water flux, and wind stress resultant from models using fixed SSTs are:

1. The discrepancies of local model results are of the same order of magnitude as the climate change from PD to LGM,
2. The model discrepancies are slightly increased for a climate state different from the modern one.
3. The anomalies between the two climate state agree much better then the states themselves.

While models with fixed SSTs exhibit significant anomalies between the time slices, the anomalies resultant from models with calculated SSTs are situated within the range of model discrepancies.

References:

Joussaume, S., and K.E. Taylor, 1995: Status of the "Paleoclimate Modelling Intercomparison Project" (PMIP). *Proceedings of the First International AMIP Scientific Conference*, WCRP Report **92**, 425-430.

Lorenz, S., B. Grieger, Ph. Helbig, and K. Herterich, 1996: Investigating the sensitivity of the Atmospheric General Circulation Model (ECHAM 3) to paleoclimatic boundary conditions. *Geologische Rdsch.* **85**, 513-524.

Workshop Announcement

WCRP/SCOR Workshop on Intercomparison and Validation of Ocean-Atmosphere Flux Fields

Washington DC area, USA, 21-25 May 2001

The WCRP/SCOR Workshop on Intercomparison and Validation of Ocean-Atmosphere Flux Fields, to be held in Washington DC, USA, **(21-25 May 2001),** is the second meeting encouraging interaction and dialogue between the diverse scientific communities involved in producing and using air-sea fluxes.

Following the landmark First WCRP Workshop on Air-Sea Flux Fields for Forcing Ocean Models and Validating GCMs held at ECMWF, Reading, in October 1995, a joint WCRP/SCOR Working Group on Air-Sea Fluxes was set up to continue to foster interdisciplinary consultations in this area, and to catalogue and keep under review available surface flux and flux-related data sets. The Final Report of the Working Group is a substantial document assessing the present state of the art in regard to air sea flux determination ("Intercomparison and Validation of Ocean-Atmosphere Energy Fluxes" shortly to be published in the WCRP report series). The report can be accessed at *http://www.soc.soton.ac.uk/JRD/MET/WGASF*.

Aims of the Workshop are to

- bring together the different scientific communities interested in air-sea fluxes and working on their development and application through modelling, remote sensing and in-situ measurements;
- stimulate discussion by a wide spectrum of the research community on the issues raised in the WGASF report, consider group recommendations and discuss priorities for future activities in the areas identified as significant knowledge gaps;
- consider the need for any continuing internationally coordinated initiative in air-sea flux studies.

A focus of the Workshop will be to summarize recent developments of in-situ, remotely sensed and model output fields for flux and flux related parameters. Particular attention will be devoted to assessing the uncertainties inherent in the various fields. Although primarily concerned with global-scale flux climatologies, emphasis will also be given to the development of flux parameterizations, and to field experiments and other high quality in-situ flux data, designed to refine those parameterizations. Contributions dealing with global and basin-scale energy balances, and the variability of ocean-atmosphere fluxes will also be welcome.

The workshop is intended to promote feedback and encourage dialogue between the producers and users of surface flux and related data. Following an introductory presentation of the WGASF report, sessions will address the key topics using a combination of invited, oral and poster papers. Break-out groups will be tasked with considering an effective and balanced strategy for making further progress in the study and utilization of ocean-atmosphere fluxes.

The organisers of the workshop (Frank Bradley, Sergey Gulev - organizing committee chair, David Legler - local organizing committee chair, Roger Newson, Jörg Schulz, Peter Taylor, and Glenn White) are pleased to invite all interested scientists to send statements of interest, abstracts of papers (if you are going to present one) and submittal information (name, address, e-mail, telephone, fax).

Note, that all information should be sent on e-mail, mail or fax by the deadline of **15 January 2001** to Sergey Gulev (P.P.Shirshov Institute of Oceanology, RAS, 36 Nakhimovsky ave., 117851, Moscow, Russia, Email: gul@gulev.sio.rssi.ru, fax: +7-095-1245983, tel: +7-095-1247985).

Further information about the Workshop will be available shortly at *http://www.soc.soton.ac.uk/JRD/MET/WGASF.*

CLIVAR Calendar

2000/2001	Meeting	Location	Attendance
October 4-6	WGCM Workshop on Decadal Predictability	La Jolla, USA	Open
October 9-11	JSC/CLIVAR Working Group on Coupled Modelling	La Jolla, USA	Invitation
October 9-12	Workshop on "Shallow Tropical-subtropical Overturning Cells and their Interaction with the Atmosphere"	Venice, Italy	Open
October 17-20	WOCE/CLIVAR Representativeness and Variability Workshop	Fukuoka, Japan	Open
October 23-27	25th Climate Diagnostics and Prediction Workshop	Palisades, USA	Open
October 23-27	CAS/JSC WG on Numerical Experimentation	Melbourne, Australia	Invitation
November 1-3	CLIVAR Working Group on Seasonal to Interannual Prediction	Buenos Aires, Argentina	Invitation
November 13-15	Sustained Observations for Climate of the Indian Ocean	Perth, Australia	Invitation
November 16-17	TAO Implementation Panel, 9th Session	Perth, Australia	Invitation
November 16-18	CLIVAR Southern Ocean Workshop	Perth, Australia	Invitation
November 28-December 1	Chapman Conference on the North Atlantic Oscillation	Ourense, Spain	Open
December 1-2	CLIVAR Atlantic Implementation Panel, 2nd Session	Ourense, Spain	Invitation
December 15-19	AGU Fall Meeting	San Francisco, USA	Open
January 8-12	NASA/IPRC Workshop on Decadal Climate Variability	Honolulu, USA	Open
January 14-19	American Meteorological Society, 81th Annual Meeting	Albuquerque, USA	Open
January 22-25	CLIVAR Pacific Implementation Workshop	Honolulu, USA	Invitation
March 12-16	Intl. Meeting of Statistical Climatology	Lüneburg, Germany	Open
March 26-30	European Geophysical Society XXVI Annual Meeting	Nice, France	Open
May 14-18	CLIVAR Scientific Steering Group, 10th Session	Toulouse, France	Invitation
May 21-25	WCRP/SCOR Workshop on Intercomparison and Validation of Ocean-Atmosphere Flux Fields	Washington DC, USA	Open
May 29-June 2	AGU Spring Meeting	Boston, USA	Open
June 25-29	WOCE/JGOFS Ocean Transport Workshop	Southampton, UK	Open

Check out our Calendar under: ***http://clivar-search.cms.udel.edu/calendar/default.htm*** *for additional information*

Contents

In this issue

The CLIVAR Newsletter Exchanges is published by the International CLIVAR Project Office.

ISSN No.: 1026 - 0471

Editors: Andreas Villwock and John Gould

Layout: Andreas Villwock

Printed by: Technart Ltd., Southern Road, Southampton SO15 1HG, UK.

CLIVAR Exchanges is distributed free-of-charge upon request (icpo@soc.soton.ac.uk).

If undelivered please return to:

International CLIVAR Project Office
Southampton Oceanography Centre, Empress Dock, Southampton, SO14 3ZH, United Kingdom